DEVELOPMENT OF A DESIGN PARAMETER FOR THE UTILIZATION OF EXHAUST GAS ENERGY OF A TWO-STROKE DIESEL ENGINE

ROBERT W. WITTER
AND
JOHN F. LOBKOVICH

DEVELOPMENT OF A DESIGN PARAMETER
FOR THE
UTILIZATION OF EXHAUST GAS ENERGY
OF A
TWO-STROKE DIESEL ENGINE

by

ROBERT W. WITTER, LIEUTENANT, UNITED STATES COAST GUARD
B.S., United States Coast Guard Academy
(1951)

and

JOHN F. LOBKOVICH, LIEUTENANT, UNITED STATES COAST GUARD
B.S., United States Coast Guard Academy
(1952)

SUBMITTED TO THE
DEPARTMENT OF NAVAL ARCHITECTURE AND MARINE ENGINEERING
on
26 May 1958
IN PARTIAL FULFILLMENT OF THE REQUIREMENTS FOR THE
DEGREE OF NAVAL ENGINEER
and
DEGREE OF MASTER OF SCIENCE
IN NAVAL ARCHITECTURE AND MARINE ENGINEERING
at the
MASSACHUSETTS INSTITUTE OF TECHNOLOGY

ABSTRACT

DEVELOPMENT OF A DESIGN PARAMETER FOR THE UTILIZATION OF EXHAUST GAS ENERGY OF A TWO-STROKE DIESEL ENGINE

by

Robert W. Witter, Lieutenant, U.S. Coast Guard

John F. Lobkovich, Lieutenant, U.S. Coast Guard

Submitted to the Department of Naval Architecture and Marine Engineering on 26 May 1958 in partial fulfillment of the requirements for the degree of Naval Engineer and degree of Master of Science in Naval Architecture and Marine Engineering.

Examination and evaluation of available exhaust-gas energy and operating performance of a two-stroke General Motors 71 series, diesel engine led to the development of dimensionless parameters, related as a single line function, to be used in design and performance estimates of two-stroke engines.

Thrust measurements were made of the exhaust gases impinging on a flat target plate for a GM3-71 laboratory engine with a single active cylinder. Two nozzles, having ratios of nozzle area to piston area equal to 0.025 and 0.05, were investigated. Indicated engine power was determined from pressure indicator cards. Flow coefficients of the GM-71 engine were determined for the two-valve and four-valve heads and the figure-8 cylinder liner.

A comparison of effective exhaust-gas velocity was made to check the correlation of two-stroke diesel engine exhaust energy utilization to that of four-stroke spark-ignition engines. It was found that two-stroke experimental results were not independent of nozzle area.

Thesis Supervisor: C. F. Taylor, Professor, Mechanical Engineering

Cambridge, Massachusetts
May 26, 1958

Secretary of the Faculty
Massachusetts Institute of Technology
Cambridge 39, Massachusetts

Dear Sir:

The attached thesis entitled "Development of a Design Parameter for the Utilization of Exhaust Gas Engery of a Two-Stroke Diesel Engine" is herewith submitted in partial fulfillment of the requirements for the degree of Naval Engineer and degree of Master of Science in Naval Architecture and Marine Engineering.

Respectfully,

ACKNOWLEDGEMENTS

The authors would like to express their appreciation for the aid and advice given them by the faculty and staff of the Sloan Automotive Laboratory of the Institute.

Particular credit and thanks are given to Professor C. F. Taylor for his help, suggestions and criticism without which this work would not have been possible.

TABLE OF CONTENTS

LIST OF SYMBOLS

A_p	Piston Area (in^2)
A_n	Nozzle Area (in^2)
$BMEP_c$	Corrected value of brake mean effective pressure (psi)
$BMEP_M$	Measured brake mean effective from dynamometer (psi)
F	Fuel air ratio based on air trapped in cylinder (dimensionless)
F'	Overall fuel air ratio (dimensionless)
FMEP	Measured friction mean effective pressure for 3 cylinders (psi)
$FMEP_c$	Corrected friction mean effective pressure for 1 cylinder (psi)
IMEP	Engine indicated mean effective pressure as determined from indicator card (psi)
K	Flow coefficient (dimensionless)
K_m	Mean value of flow coefficient (dimensionless)
$\dot{M}$ chart	Uncorrected air flow rate through ASME square edge orifice (lb/sec)
$\dot{M}_{cor}$	Corrected air flow rate (lb/sec)
$\dot{M}_F$	Mass flow rate of fuel (lb/sec)
$\dot{M}_T$	Total mass flow rate ($\dot{M}_{cor} + \dot{M}_F$) (lb/sec)
N	Engine revolutions per minute
P_a	Barometric pressure ("H_g)
P_E	Static pressure in exhaust pipe ("H_g gage)
P_T	Static pressure in exhaust tank ("H_g gage)
P_i	Static pressure in inlet air receiver ("H_g gage)
P_1	Static pressure before flow measuring orifice ("H_g gage)
ΔP	Pressure drop across the flow measuring orifice ("H_2O gage)
R	Universal gas constant
R_s	Scavenging ratio (dimensionless)

T_E	Exhaust gas temperature in pipe (^{o}F)
T_j	Engine water jacket temperature (^{o}F)
T_1	Inlet air temperature before flow measuring orifice (^{o}F)
T	Mean time average thrust force (lb)
TMEP	Turbine mean effective pressure (psi)
V_c	Clearance Volume of cylinder (ft^3)
a	Velocity of sound in air (ft/sec)
a_E	Velocity of sound in exhaust gas (ft/sec)
u	Mean velocity of exhaust gas through the nozzle (ft/sec)
S	Piston speed (ft/min)
Z	Mach index factor (dimensionless)
$\mathbb{P}$	Engine brake horsepower
Γ	Trapping efficiency (η_s/R_s)
η'_i	Indicated thermal efficiency of engine
η_{kb}	Kinetic blow down efficiency of turbo charger
η_s	Scavenging efficiency
ρ_s	Scavenging density ($\#/ft^3$)

LIST OF FIGURES

INTRODUCTION

Certain experiments aimed at raising the power of two-stroke diesel engines by means of exhaust gas turbochargers were carried out a long time ago, but it is only in recent years that successful systems have been developed. The reason for this slow development is that in two-stroke diesel engines the conditions for pressure-charging are not as favorable as in four-stroke engines. Before pressure-charging, the cylinder must be scavenged to evacuate the exhaust gases; however, scavenging and pressure-charging must be carried out without any help from the piston.

Pressure-charging introduces more air into the cylinder than is possible under atmospheric pressure. In this way a greater quantity of fuel can be burned and thus raise the power of the engine. Instead of dissipating the energy contained in the exhaust gas by throttling in valves or ports, an obvious step was to utilize it in an exhaust-gas turbine in order to recuperate some or all of the power required to drive the scavenging air pumps. The power produced in the turbine by the exhaust gases is not always sufficient to cover the compression of the scavenging and pressure-charging air, in which case some systems employ a mechanically driven scavenging pump in series or parallel with the turbocharger.

Previous experimentation indicates generally feasability studies of turbocharging applications to certain selected commercial engines. Since the design of an exhaust-gas turbocharger is largely determined by the thermodynamic requirements of the engine, this thesis is an attempt to examine and evaluate exhaust-gas thrust measurements and

engine operating characteristics of a two-stroke diesel engine (General Motors GM-71). From this experimentation, the development of related design parameters for the practical utilization of exhaust-gas energy is proposed.

PROCEDURE

1. Experimental Arrangement.

The experimental aspect of this study was conducted on a standard General Motors 3-71 series engine. One cylinder of the engine was fitted with an exhaust pipe to which nozzles of various areas could be attached. The exhaust gases were directed to impinge on a flat plate mechanical-hydraulic force measuring apparatus. The two cylinders of the engine which were not fitted with the nozzle arrangement were modified in the following manner:

a. The inlet ports and exhaust manifold were blanked off so that there was no air flow through these cylinders.

b. The fuel rack was disconnected so that there was no fuel flow to these cylinders.

This arrangement worked satisfactorily. However, it imposed the additional problem of accurately determining the friction mean effective pressure and the brake mean effective pressure for the single active cylinder. For a discussion of this phase of the study, see Appendix E.

The experimental range of fuel-air ratios and scavenging ratios that were covered are shown in Table I.

– Table I –

Range of Experiments

Nozzle Area Ratio	Fuel-Air Ratio	Scavenge Ratio
0.05	0.0175 - 0.0420	1.10 - 2.20
0.025	0.020 - 0.0560	0.60 - 1.50

Although the engine was operated in excess of its rated value of indicated mean effective pressure, operation was satisfactory and under

no operating load did the engine appear to be laboring.

Instrumentation was accomplished so that at each operating point it was possible to measure the following experimental data:

a. Air and fuel flow

b. Inlet air and exhaust gas temperatures

c. Inlet receiver, exhaust pipe and exhaust tank pressures

d. Engine dynamometer and thrust force

e. Engine cylinder pressure as a function of crank angle

f. Engine operating conditions

In addition to the above data, typical measurements of simultaneous cylinder pressure and exhaust pipe pressure were recorded as a function of crank angle for each nozzle. These diagrams clearly indicate the dynamic conditions that exist in the exhaust pipe while the engine is operating. See Figure I for the relation of cylinder pressure and exhaust pipe pressure.

Experimentation was also conducted to determine what effect the distance between the force plate and the nozzle face would have on the thrust readings. It was found that the thrust force peaked at a distance of about 2" and was then relatively independent of distance to a distance of $4\frac{1}{2}$" when it commenced to fall off. Experimentation was run with distance from nozzle face to force plate set at $2\frac{1}{4}$".

2. Computation Procedure

The engine mean effective pressure was determined from the crank angle-pressure indicator diagrams. Engine brake horsepower was computed from the dynamometer brake load and corrected as outlined in Appendix E. Turbine mean effective pressure was determined from an equation derived on the basis that the turbine system was utilizing blow down energy of

the exhaust gases. In order to determine turbine mean effective pressure, it was necessary to make the following assumptions:

$\eta_{kb} = 0.75$ where η_{kb} is the kinetic blow down efficiency of the turbine

$\eta'_{i} = 0.46$ where η'_{i} is the indicated thermal efficiency of the engine.

These values of efficiency were taken from the best available source. All dimensionless parameters were then computed and placed on separate computation sheets so that the results may be easily verified if the reader so desires. See Appendix A for development of dimensionless parameters.

3. Presentation of Results

The experimental data was taken under two different sets of conditions for operation. On the 0.025 nozzle, the inlet pressure was maintained constant for all runs. When conducting the experimental phase of the 0.05 nozzle, the runs were conducted at essentially constant scavenging ratios. It was possible to correlate the data taken under both conditions but it was found that considerably less effort was required if the engine was operated at constant scavenge ratios.

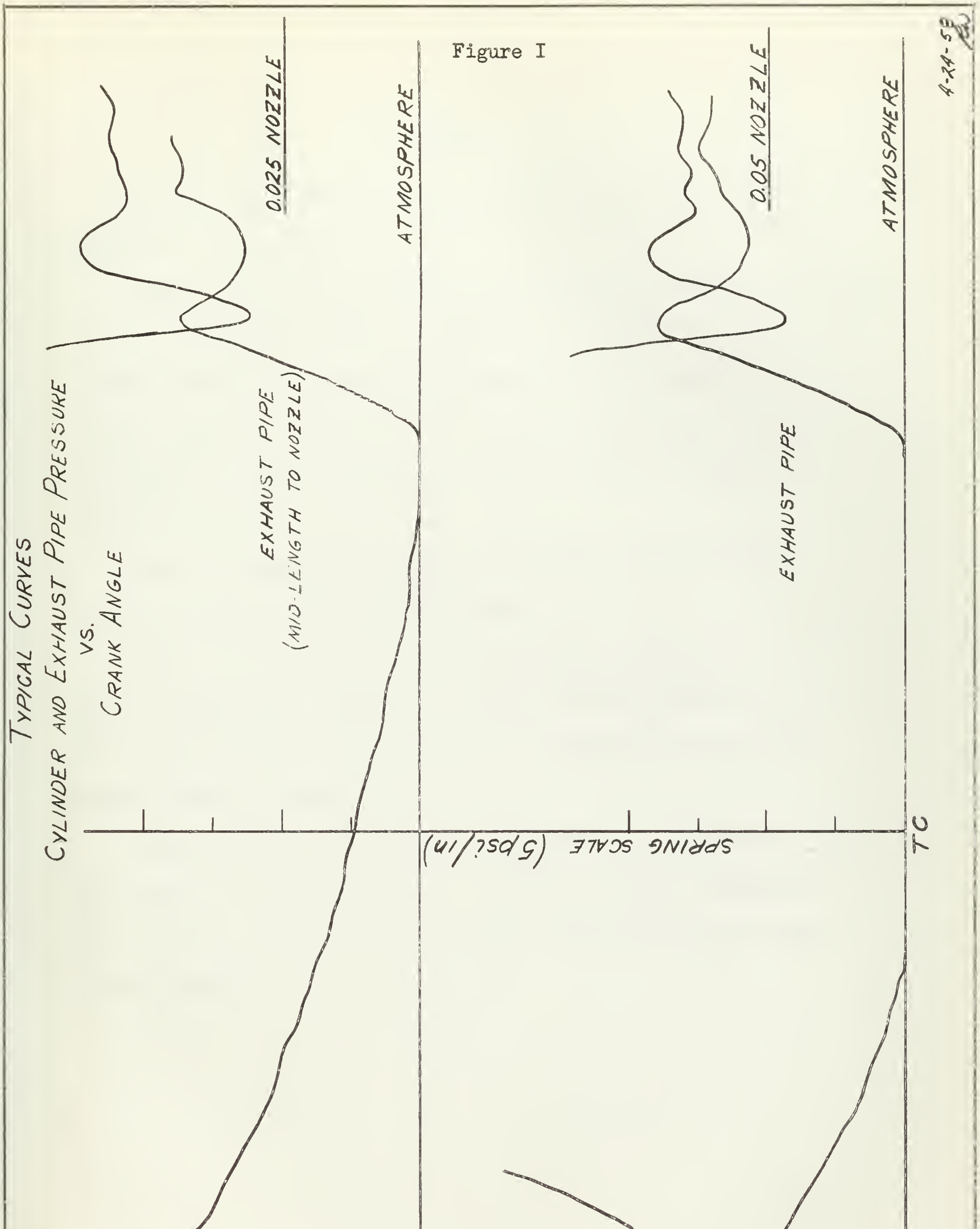
TYPICAL CURVES
CYLINDER AND EXHAUST PIPE PRESSURE
VS.
CRANK ANGLE
EXHAUST PIPE
(MID-LENGTH TO NOZZLE)
0.025 NOZZLE
ATMOSPHERE
0.05 NOZZLE
EXHAUST PIPE
ATMOSPHERE
SPRING SCALE (5 psi/in)
TC
4-24-58
Figure I

RESULTS

The results of this experimentation are presented in Figures II through VI, which follow.

Figure II presents a comparison of effective exhaust-gas velocity from a single cylinder engine. The ratio of effective gas velocity and sonic velocity at exhaust temperature is plotted against a dimensionless parameter involving nozzle downstream pressure, nozzle area, gravitational constant, total gas flow rate, and sonic velocity at exhaust temperature.

Figure III shows the dimensionless relation of exhaust-gas thrust and single cylinder engine IMEP.

Figure IV presents the dimensionless MEP relations for the utilization of exhaust-gas energy. The ratio of engine IMEP plus turbine MEP to engine IMEP is plotted against the same dimensionless IMEP parameter used in Figure III.

Figures V and VI present a dimensionless relation of thrust and brake power for the GM-71 diesel. For the 0.05 nozzle scavenging ratio was held constant and for the 0.025 nozzle inlet air pressure was held constant.

Figure II

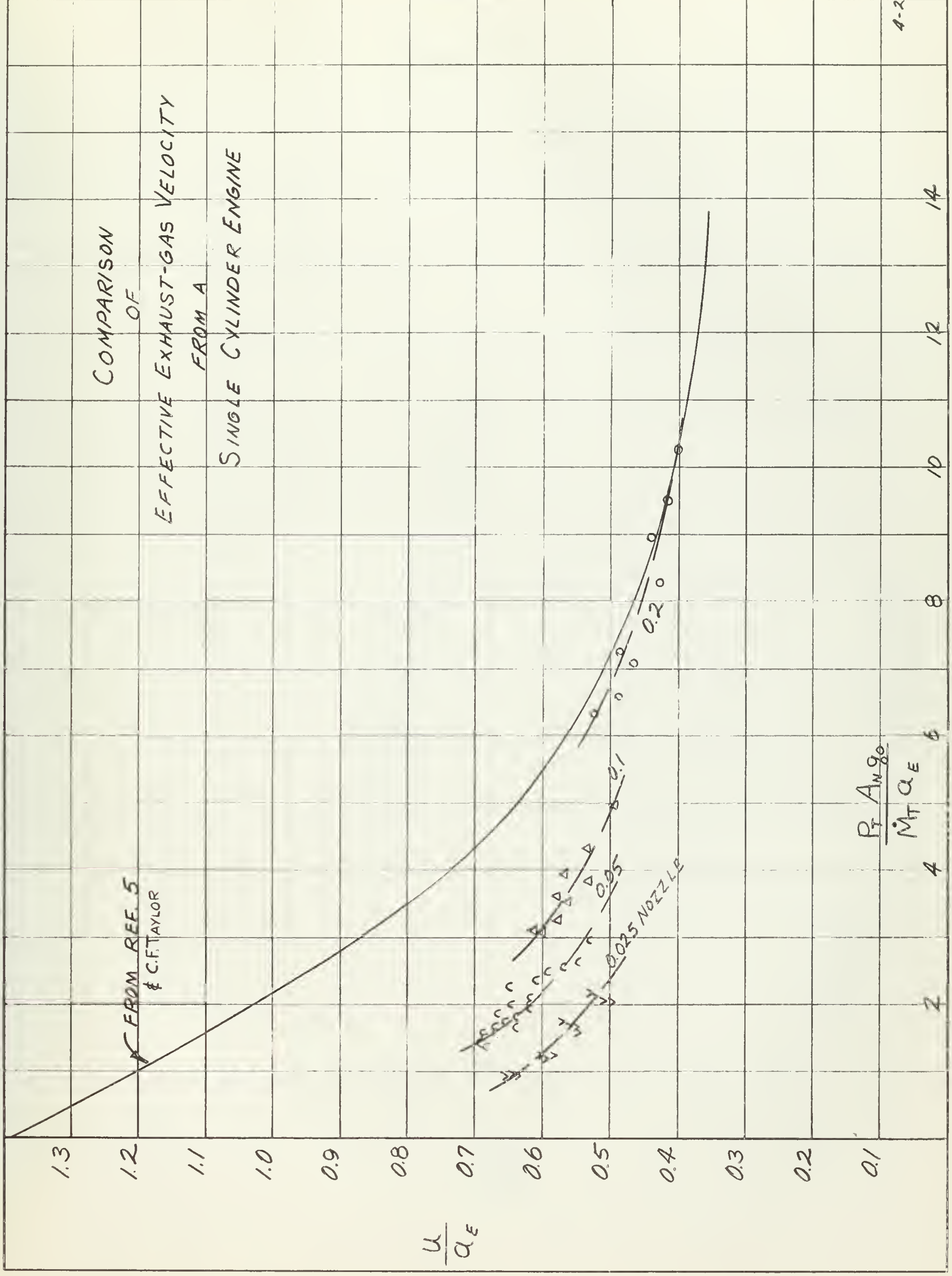

4-24-58
COMPARISON
OF
EFFECTIVE EXHAUST-GAS VELOCITY
FROM A
SINGLE CYLINDER ENGINE
FROM REF. 5
& C.F. TAYLOR
0.2
0.1
0.05
0.025 NOZZLE
$\frac{P_T A_N g_o}{\dot{M}_T a_E}$
$\frac{u}{a_E}$
1.3
1.2
1.1
1.0
0.9
0.8
0.7
0.6
0.5
0.4
0.3
0.2
0.1
2
4
6
8
10
12
14

Figure III

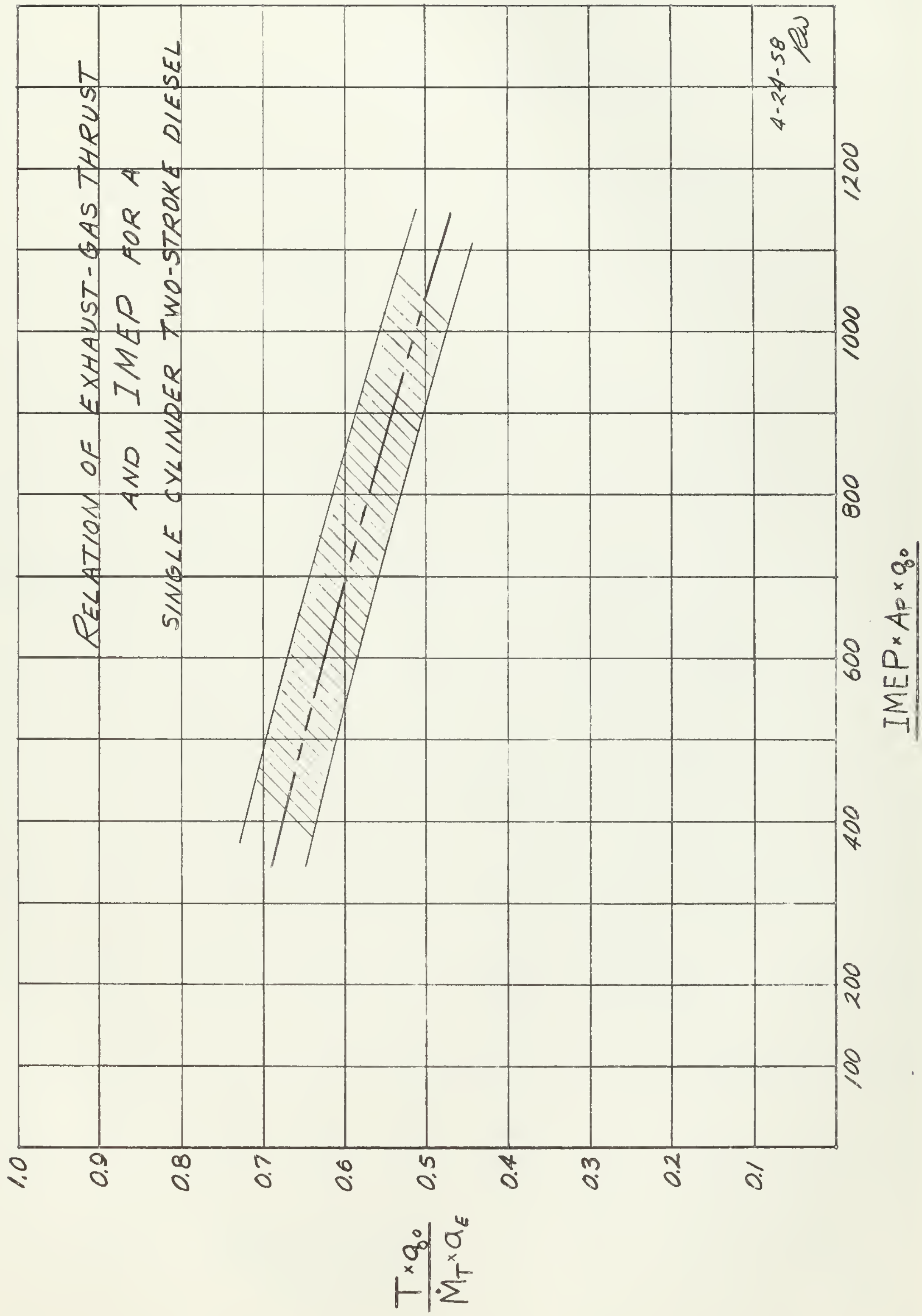
RELATION OF EXHAUST-GAS THRUST
AND IMEP FOR A
SINGLE CYLINDER TWO-STROKE DIESEL
4-24-58
$\frac{IMEP \times A_P \times g_o}{\dot{M}_T \times a_E}$
$\frac{T \times g_o}{\dot{M}_T \times a_E}$
100 200 400 600 800 1000 1200
1.0 0.9 0.8 0.7 0.6 0.5 0.4 0.3 0.2 0.1

Figure IV

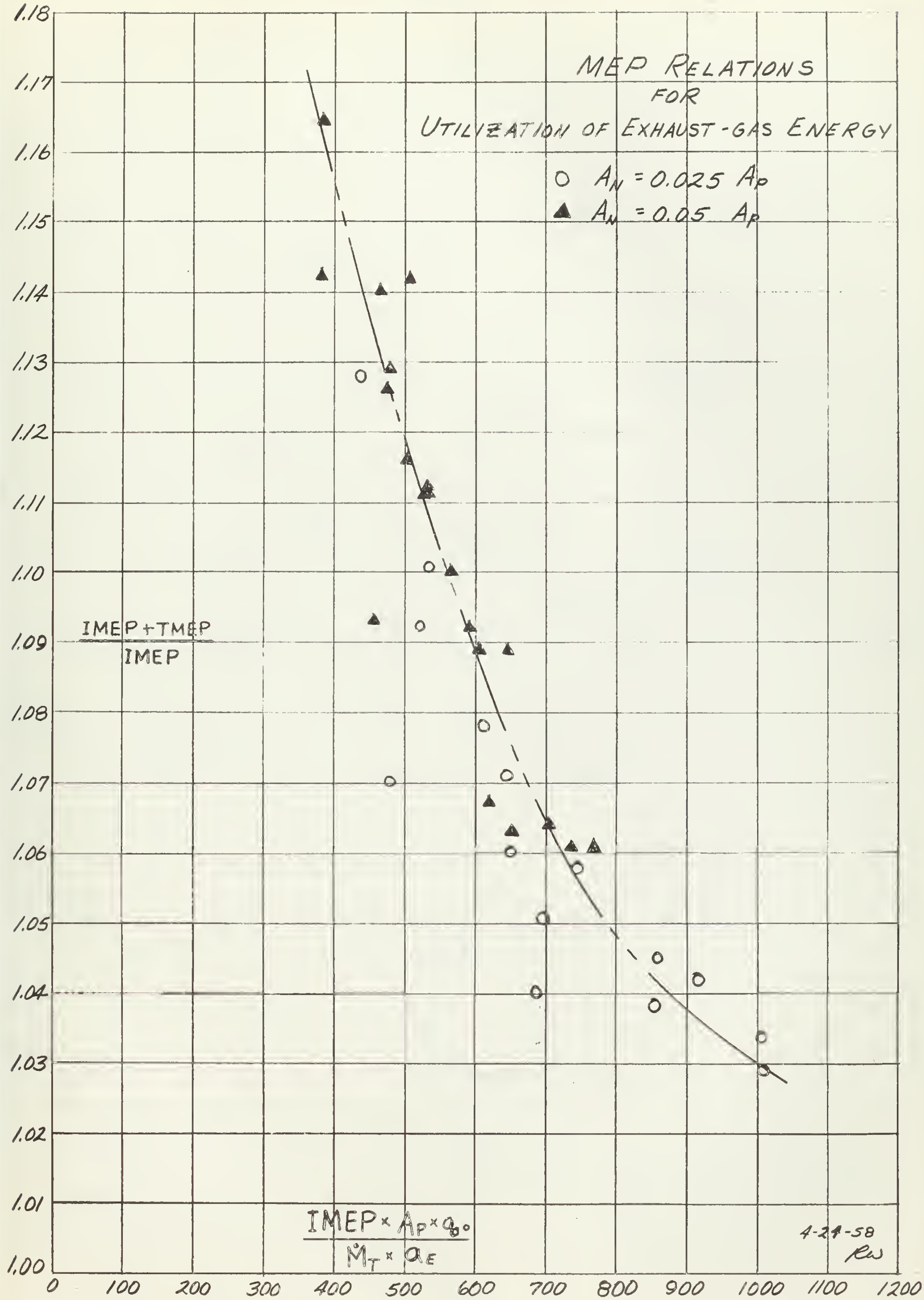

MEP RELATIONS
FOR
UTILIZATION OF EXHAUST-GAS ENERGY
○ $A_N = 0.025\ A_P$
▲ $A_N = 0.05\ A_P$
$\frac{IMEP + TMEP}{IMEP}$
$\frac{IMEP \times A_P \times a_0}{\dot{M}_T \times a_E}$
1.18
1.17
1.16
1.15
1.14
1.13
1.12
1.11
1.10
1.09
1.08
1.07
1.06
1.05
1.04
1.03
1.02
1.01
1.00
0
100
200
300
400
500
600
700
800
900
1000
1100
1200
4-24-58
RW

Figure V

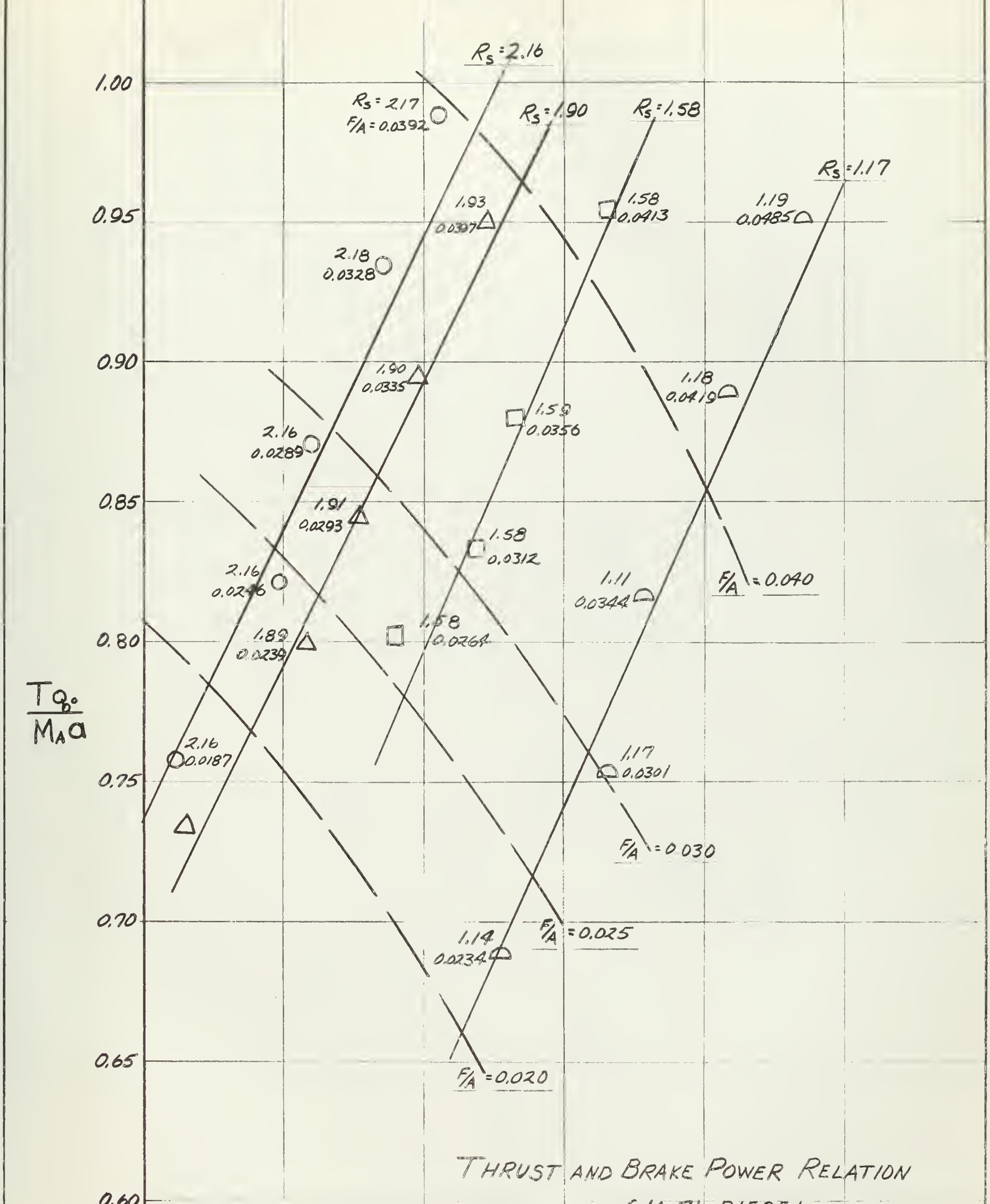
THRUST AND BRAKE POWER RELATION
GM-71 DIESEL
NOZZLE : 0.05
R_s = 2.16
R_s = 1.90
R_s = 1.58
R_s = 1.17
F/A = 0.040
F/A = 0.030
F/A = 0.025
F/A = 0.020
R_s = 2.17 F/A = 0.0392
2.18 0.0328
2.16 0.0289
2.16 0.0246
2.16 0.0187
1.93 0.0397
1.90 0.0335
1.91 0.0293
1.89 0.0239
1.58 0.0413
1.59 0.0356
1.58 0.0312
1.58 0.0261
1.19 0.0485
1.18 0.0419
1.11 0.0344
1.17 0.0301
1.14 0.0234
1.00
0.95
0.90
0.85
0.80
0.75
0.70
0.65
0.60
2
3
4
5
6
7
$\frac{Tq_{b_0}}{M_A a}$
$\frac{Pq_{b_0}}{M_A a^2}$
1-28-58

Figure VI

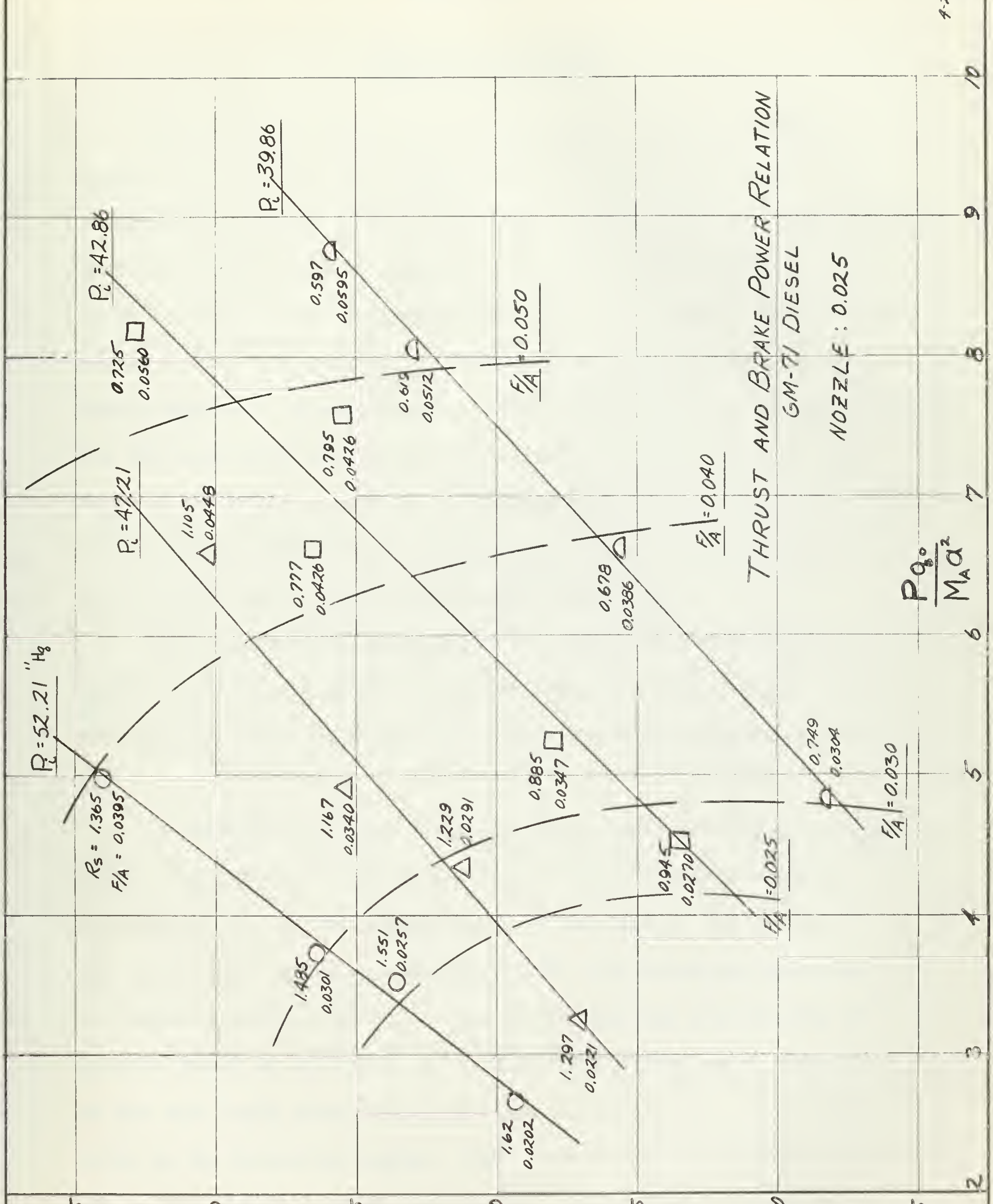
THRUST AND BRAKE POWER RELATION
GM-71 DIESEL
NOZZLE : 0.025
P_c = 52.21 "Hg
P_c = 47.21
P_c = 42.86
P_c = 39.86
R_S = 1.365
F/A = 0.0395
F/A = 0.025
F/A = 0.030
F/A = 0.040
F/A = 0.050
$\frac{Pg_0}{M_A a^2}$
$\frac{Tg_0}{M_A a}$

DISCUSSION OF RESULTS

The comparison of effective exhaust-gas velocity presented in Figure II was made at the suggestion of the thesis supervisor. The original test results of reference (5) were from a single cylinder spark-ignition aircraft engine operated over a wide range of engine speeds, inlet manifold pressures, exhaust pressures, and nozzle areas and were plotted close to a common line. However, experimental data of this thesis separated, though within a fairly uniform band, to distinct regions for the respective nozzles and were below the common line indicated. Variance of fuel-air ratio and scavenging ratio had no evidenced effect. These results occurred in the region where high gas velocity (high exhaust thrust) utilization would be most significant.

This finding may be attributed to the larger overall air-fuel flow rate of the diesel engine which overbalances the lower exhaust temperature effects resulting from the method of cylinder charging and scavenging.

In general, it may be concluded that exhaust-gas thrust increases with a reduction in nozzle area until a critical area is reached.[2,5] The optimum size is the one resulting in the largest sum of engine MEP plus turbine MEP minus compressor MEP. The relations presented in Figures V and VI also show, upon comparison, the availability of greater thrust by utilizing the smaller 0.025 nozzle under conditions of the same brake power, inlet air flow, scavenge ratio, and fuel-air ratio in the laboratory engine. This finding further emphasizes the generally known fact that to effectively supercharge a two-stroke engine, it is necessary to raise the exhaust pressure by some means.

Figures V and VI, involving brake power relationships, are somewhat limited in their usefulness except when comparing the laboratory engine under varied operating conditions.

The results presented in Figures III and IV are considered most useful for design purposes. Indicated MEP relations provide a better basis for comparison and correlation of engines of differing characteristic geometry and operating conditions. The use of Figure IV in conjunction with basic (i.e., preliminary) design analysis should broaden the scope of performance estimates of two-stroke engines.

Analysis of data, such as $\frac{IMEP + TMEP}{IMEP}$ at thrust parameter, as a function of $^{P}E/_{P_i}$ should give additional information as to nozzle area and exhaust pressure level for supercharging of two-stroke engines.

The practicability of pressure-charging by means of an exhaust-gas turbocharger alone was not investigated for this engine. Such analysis would be of interest.

In a blow-down method of exhaust-gas energy utilization, the length and diameter of exhaust pipe to the turbine nozzle would appear to be of some importance. These effects were considered but not investigated.

CONCLUSIONS AND RECOMMENDATIONS

CONCLUSIONS

1. It was not possible to correlate the utilization of exhaust gas energy of a two-stroke diesel engine as a single line function with the parameters that were developed for single cylinder tests using aircraft engines. Although qualitative correlation to the data of Pinkel(5) was obtained, the experimental results of this thesis indicated that the effective gas velocity relations were not independent of nozzle area.

2. Correlation of the dimensionless parameters $\frac{T_{go}}{M_T\ a_E}$ and $\frac{IMEP + TMEP}{IMEP}$ to $\frac{IMEP \times A_p \times go}{M_T\ a_E}$ as a single line function is possible for use in design and performance estimates of two-stroke engines.

3. Exhaust-gas thrust increases with a reduction of nozzle area.

RECOMMENDATIONS

1. Analysis of MEP and thrust relations as a function of P_E/P_i should be conducted to give additional information as to nozzle area effects and exhaust pressure level for the supercharging of two-stroke engines.

2. The experimental data should be further extended to determine the practicability of pressure-charging with an exhaust-gas turbocharger alone. Plotting $\frac{IMEP + TMEP - CMEP}{IMEP}$ as a function of the parameter indicated in Figure IV would provide an additional useful design instrument.

3. For further experimentation:

   a. investigate the effects of exhaust pipe length and diameter in the utilization of blow-down energy and the influence of length and diameter on the design functions developed in this thesis.

   b. using other two-stroke engines, including opposed-piston, check the developed design parameters.

   c. operate the laboratory GM-71 engine at constant values of scavenge ratio (R_s) for ease of operation and interpretation of results.

APPENDICES

APPENDIX A

Development of Dimensionless Parameters

The use of the methods of dimensional analysis has long been recognized as a valid and extremely useful experimental technique. The number of factors controlling a physical system, such as a diesel engine and turbocharger system, are many and it is only by the use of dimensional analysis that experimentation can be logically planned and the results accurately interpreted.

By holding all dimensionless groups essentially constant, except one, it was possible to examine the effect of that parameter in relation to the physical system. The experimental phase of this thesis was conducted with the exhaust thrust force (T) being the dependent variable while the independent variables were F, R_s, P_E/P_i, s/a, A_N/A_p.

Since these factors controlling the investigated system are extremely complex, it was felt that the dimensionless parameters developed for the presentation of the experimental results are the ones most useful in the consideration of basic design and performance estimates of two-stroke engines.

APPENDIX B

1. Establishment of Engine Test Operating Conditions

It was determined from reference (2) that operation of the GM71 series engine at rated speed (1600 rpm) gave unsatisfactory flow characteristics when examining the engine under supercharged conditions. In order to approximate the flow characteristics under supercharged conditions, it was attempted to duplicate the dynamic flow conditions of the turbo-charged GM71T series engine with the laboratory GM71 series engine. It was felt that operation of the engines at the same Mach index factors would give essentially the same flow characteristics.

To establish the Mach index factors, it was necessary to determine the steady state flow coefficients of

(a) GM71 series cylinder head (2 exhaust valves)

(b) GM71T series cylinder head (4 exhaust valves)

(c) cylinder liners (intake ports)

Using the mean steady state flow coefficients which were found experimentally, it was possible to calculate an overall mean steady state flow coefficient for the engine as a complete unit.

The above procedures were followed. It was determined that in order to duplicate the Mach index factor of the turbo-charged engine, it would be necessary to operate the laboratory engine at 1285 rpm. However, realizing that the dynamic engine conditions cannot be exactly duplicated and represented by steady state conditions, the decision was made to operate the engine at 1200 rpm. Operation of the engine at this speed did give satisfactory results for the analysis of exhaust gas energy utilization.

2. List of Symbols

A	orifice area	(in^2)
C	mean steady state dimensionless flow coefficient	
D_2	orifice diameter	(in)
G	specific gravity of air (1.0)	
K	dimensionless flow coefficient	
$\dot{M}$	air mass flow rate (lb/sec)	
$\dot{M}_{cor}$	corrected air mass flow rate (lb/sec)	
$\dot{M}_{calc}$	air mass flow rate calculated from compressible flow theory (lb/sec)	
P_1	static pressure before orifice ("H_g abs)	
P_2	static pressure after orifice	
ΔP_o	pressure drop across orifice ("H_2O)	
ΔP_e	pressure drop across exhaust valves ("H_2O)	
ΔP_i	pressure drop across inlet ports ("H_2O)	
R_d	Reynolds number	
Y	expansion factor	
Z	Mach index factor (dimensionless)	
a	velocity of sound in air (ft/sec)	
s	piston speed (ft/min)	
y	super compressibility factor	
ρ	density of air (lb/ft^3)	
ϕ	compressible flow function (dimensionless)	
μ	viscosity of air (lb/ft sec)	

Subscripts

i	inlet
e	exhaust
o	stagnation
a	atmospheric

3. Determination of Air flow rate through ASME square edge orifices with flanged taps.

From reference (4)

Orifice equation:

$$\dot{M} = 0.1145 \; D_2^{\,2} \; KY \sqrt{\frac{P_1}{T_1} \; Gy \; \Delta P_o} \tag{1}$$

The flow coefficient (K) has been found to be a function of two quantities, i.e., the "discharge coefficient" and the "velocity of approach factor."

$$K = \frac{C}{\sqrt{1-B^4}} \qquad \text{where } B = {}^{D_2}/_{D_1} = \frac{1.227}{3.0} = 0.408$$

the expansion factor (Y) may be determined by the following equation:

$$Y \quad 1 - \left[0.41 \quad 0.35 \left(\frac{D_2}{D_1}\right)^4\right] \quad \left[\frac{\Delta P_o}{P_1} \quad x \quad {}^1/_{K_1}\right]$$

where $K_1 = \dfrac{C_p}{C_v}$

Expansion factors for air may be found in reference (4).

Assuming G & y = 1.0 (this does not introduce any appreciable error) equation (1) then reduces to

$$\dot{M} = K_2 K_m \; {}^K/_{K_m} \quad Y \sqrt{\frac{P_1}{T_1} \; \Delta P_o} \tag{1a}$$

$$K_2 = 0.1145(1.227)^2$$

where K_m = mean value of K (determined from table 6 reference (4))

$$K_m = 0.6150$$

then $$\dot{M} = 0.106 \;\; {}^K/_{K_m} \quad Y \sqrt{\frac{P_1}{T_1} \; \Delta P_o} \tag{1b}$$

Since K is a function of Reynolds number and B, a trial and error solution is necessary. This procedure may be simplified by assuming

$${}^K/_{K_m} = 1.0$$

$$R_d = \frac{15.28\ \dot{M}}{D_2} \tag{2}$$

Solving equation (1b) for $\dot{M}$, the Reynolds number may be found. Using this value of R_d, determine K from table (1), reference (4).

The mass flow rate is then corrected in the following manner -

$$\dot{M}_{cor} = \dot{M}\ ({}^{K}/_{K_m}) \tag{3}$$

4. Determination of steady state flow conditions.

Since it is unknown if any pressure recovery will take place through the exhaust valves, this analysis is based upon compressible flow theory.

$$\dot{M}_{calc} = A\ a_{o'}\ \rho_{o'}\ \phi \tag{4}$$

$$\phi = \sqrt{\frac{2}{K-1}\ (r^{\ 2/k} - r^{\ k+1/k})}$$

$$r = {}^{P_2}/_{P_{o'}} \qquad K = {}^{C_p}/_{C_v}$$

The flow coefficient C is defined as

$$C = \frac{\text{measured air mass flow}}{\text{calculated air mass flow}} \qquad \frac{\dot{M}_{cor}}{A\ a_{o'}\ \rho_{o'}\ \phi} \tag{5}$$

$$CA = \frac{\dot{M}_{cor}}{a_{o'}\ \rho_{o'}\ \phi} \tag{6}$$

$$T_{o'} = 70.9\ {}^{o}F = 530.9\ {}^{o}R$$

$$a_{o'} = 49\ \sqrt{T_{o'}} = 1131\ fps$$

$$\rho_{o'} = \frac{P_{o'}}{R\ T_{o'}} = \frac{2118}{53.35 \times 530.9} = 0.0749\ lb/ft^3$$

$$CA = \frac{\dot{M}_{cor} \times 144}{0.0749 \times 1131 \times \phi} = 1.71\ \frac{\dot{M}_{cor}}{\phi} \tag{7}$$

The factor $\frac{CA}{A_p}$ was plotted versus crank angle through the range that exhaust valves and inlet ports are open. From this plot, the mean value of $\frac{CA}{A_p}$ was determined by integration of the area under the curves and dividing by the respective abscissa of crank angle opening duration. Therefore, also, the mean C_e and mean C_i for each type cylinder head and liner was determined by applying the appropriate value of A and A_p as follows:

piston area, A_p = 14.15 in.^{2}

two-valve, A_e = 2.4 in.^{2} (max.)

four-valve, A_e = 2.65 in.^{2} (max.)

figure - 8, A_i = 5.7 in.^{2} (max.)

See figure VII, Inlet and Exhaust Flow Coefficients; relations of valve lift and piston position to crank angle were established from measurements taken on the laboratory GM-71 engine.

5. Calculation of the mean overall steady state flow coefficient for the engine.

Schematic engine diagram

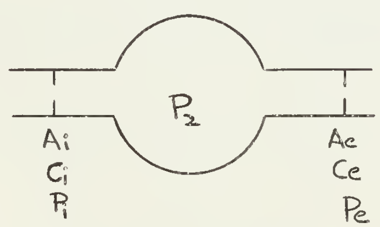

Figure VII

4-25-58
RW

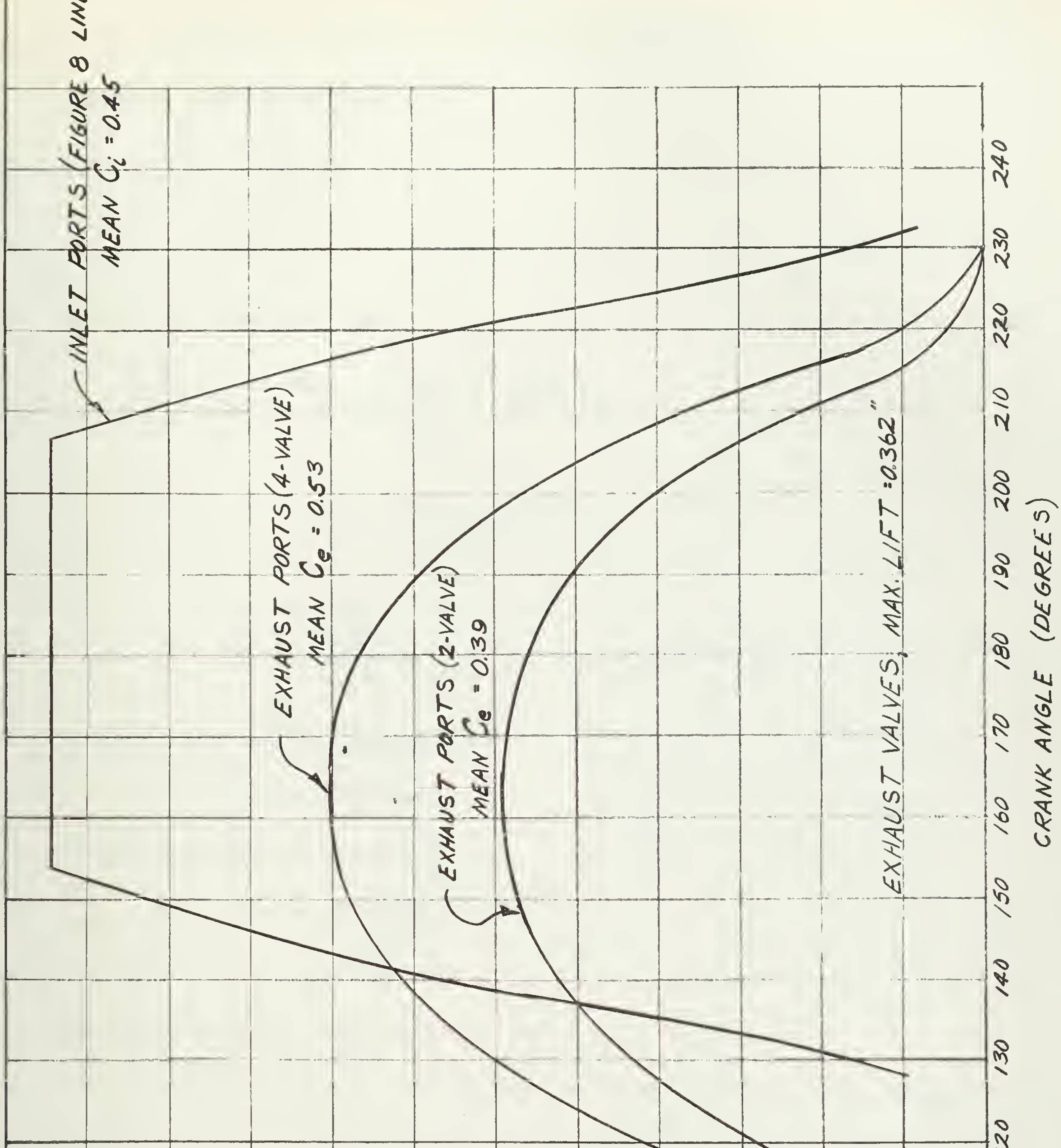

INLET AND EXHAUST FLOW COEFFICIENTS (GM-71)

$$\dot{M} = C_i A_i \rho_i a_i \ \phi(P_2/P_i) = C_e A_e \rho_2 a_e \ \phi(P_e/P_2) \tag{8}$$

Assuming adiabatic flow of a perfect gas -

$$\frac{\rho_2}{\rho_i} = \frac{P_2}{P_i} \qquad T_i = T_2 = T_e$$

$$a_i = a_e$$

It follows therefore that

$$\phi\left(P_2/P_i\right) = \frac{\rho_2}{\rho_i} \times \frac{A_e C_e}{A_i C_i} \times \phi\left(P_e/P_2\right)$$

$$\phi\left(P_2/P_i\right) = P_2/P_i \times \frac{A_e C_e}{A_i C_i} \times \phi\left(P_e/P_2\right) \tag{9}$$

$$\frac{P_e}{P_2} = \frac{P_e/P_i}{P_2/P_i}$$

Defining the overall condition as

$$\dot{M} = CA\rho_i a \ \phi\left(P_e/P_i\right) \tag{10}$$

Equating equations 8 and 10

$$CA = C_i A_i \ \frac{\phi\left(P_2/P_i\right)}{\phi\left(P_e/P_i\right)} \tag{11}$$

Equations 9 and 10 must be satisfied simultaneously.

The solution to these equations may be found on figure 7-14 reference (11).

Figure 7-14, "Flow Through Orifices in Series", relates C/C_i vs $\frac{C_e A_e}{C_i A_i}$ at constant values of P_e/P_i .

6. Engine Test Operating Conditions.

The Mach index factor (Z) is defined as

$$Z = \frac{\text{characteristic engine area}}{\text{characteristic flow area}} \times \frac{S}{C_a}$$

For this analysis - C x characteristic flow area will be defined as the mean overall steady state value found from paragraph 5. Since the characteristic engine area is the same for both engines:

$$\left(\frac{S}{CA_i}\right)_{GM3-71} = \left(\frac{S}{CA_i}\right)_{GM3-71T}$$

For the GM71 series engine

$N = 1600$ rpm

$A_i = 5.7$ in^2

$C_i = 0.45$ (mean value of C_i determined from flow analysis)

$\frac{C_e A_e}{C_i A_i} = 0.474$ (Determined from flow analysis)

from figure 7-14 using $\frac{C_e A_e}{C_i A_i} = 0.474$ as an entering argument

$C/C_i = 0.44$

$C = 0.44\, C_i = 0.198$

$CA_i = 0.198 \times 5.7 = 1.128$

For the GM71T series engine

$N = 2300$ rpm

$A_i = 7.9$ in^2

$\frac{A_e}{A_i} = 0.476$

Due to the fact that the liner flow characteristics on this engine were not available, it was necessary to assume that the ratio of $\frac{C_e}{C_i}$ would be approximately the same as that found experimentally for the series 71 engine.

Based on this assumption then

$$\frac{C_i}{C_e} = 1.152 \qquad \frac{C_e A_e}{C_i A_i} = 0.413$$

$$C/C_i = 0.42 \qquad C = 0.42(0.611) = 0.256$$

$$CA_i = 0.256 \times 7.9 = 2.02$$

$$\left(\frac{N}{CA_i}\right)_{71} = \left(\frac{N}{CA_i}\right)_{71T}$$

$$N_{71} = \frac{2300 \times 1.128}{2.02} = 1285 \text{ rpm}$$

In view of the assumption necessary to find CA_i for the series 71T engine and also due to the fact that static flow conditions will not duplicate dynamic engine operating conditions, the decision was made to operate the engine at 1200 rpm.

APPENDIX C

SUMMARY OF DATA AND COMPUTATIONS

COMPUTATION SHEET STEADY STATE FLOW COEFFICIENTS

Series 71T Cylinder Head (4 valve)

Lift	ΔP_o	P_1	$\Delta P_o/P_1$	Y	$\sqrt{\frac{P_1}{T_1}\Delta P_o}$	$\dot{M}$	$R_d x10^{-5}$	K/K_m	$\dot{M}_{cor}$	ΔP_e	P_2	P_2/P_a	ϕ
0	0	363.9	0	1.0	0	0	0	1.0	0	39.9	365.1	0.903	0.353
0.05	16.7	377.0	0.0443	0.986	0.922	0.0965	0.973	0.996	0.0960	26.8	378.2	0.935	0.291
0.10	30.4	388.6	0.0782	0.976	1.287	0.1332	1.345	0.994	0.1324	14.3	390.7	0.965	0.220
0.15	35.7	395.3	0.0904	0.972	1.406	0.1448	1.462	0.994	0.1439	9.3	395.7	0.977	0.180
0.20	38.0	395.5	0.0960	0.971	1.450	0.1491	1.501	0.993	0.1481	7.1	397.9	0.984	0.149
0.25	39.3	396.4	0.0992	0.970	1.476	0.1518	1.532	0.993	0.1505	6.0	399.0	0.985	0.142
0.30	40.2	397.2	0.101	0.969	1.492	0.1532	1.547	0.993	0.1520	5.2	399.8	0.988	0.128
0.35	40.6	397.5	0.1024	0.969	1.506	0.1546	1.560	0.993	0.1532	4.8	400.2	0.989	0.122
0.40	40.8	397.8	0.1026	0.969	1.506	0.1546	1.560	0.993	0.1532	4.5	400.5	0.990	0.116
0.45	41.0	398.0	0.1030	0.969	1.510	0.1552	1.568	0.993	0.1540	4.3	400.7	0.990	0.116
0.50	41.3	398.2	0.1036	0.968	1.510	0.1551	1.567	0.993	0.1540				

P_a = 405" H_2O

COMPUTATION SHEET STEADY STATE FLOW COEFFICIENT

Series 71 Cylinder Head (2-valve)

Lift	ΔP_o	P_1	$\Delta P_o/P_1$	Y	$\sqrt{\frac{P_1}{T_1}\Delta P_o}$	$\dot{M}$	$R_d \times 10^{-5}$	K/K_m	$\dot{M}_{cor}$	ΔP_e	P_2	P_2/P_a	ϕ
0	0	364.3	0	1.0	0	0	0	1.0	0	40.2	364.8	0.904	0.353
0.05	6.6	368.9	0.0179	0.995	0.584	0.0616	0.621	0.998	0.0612	35.5	369.5	0.915	0.332
0.10	19.0	378.8	0.0502	0.984	1.00	0.1042	1.053	0.995	0.1020	24.9	380.1	0.938	0.286
0.15	28.3	386.7	0.0732	0.978	1.257	0.1302	1.316	0.994	0.1263	16.4	388.6	0.960	0.234
0.20	33.5	391.3	0.0856	0.974	1.352	0.1398	1.411	0.994	0.1350	11.5	393.5	0.970	0.204
0.25	36.4	393.8	0.0925	0.972	1.412	0.1452	1.468	0.994	0.1401	8.9	396.1	0.976	0.183
0.30	37.9	395.1	0.0959	0.971	1.441	0.1483	1.500	0.993	0.1431	7.5	397.5	0.980	0.166
0.35	38.5	395.6	0.0974	0.970	1.460	0.1500	1.515	0.993	0.1446	6.9	398.1	0.981	0.162
0.40	38.9	395.9	0.0983	0.970	1.464	0.1505	1.520	0.993	0.1449	6.6	398.4	0.982	0.158
0.45	39.1	396.1	0.0987	0.970	1.470	0.1512	1.528	0.993	0.1458	6.4	398.6	0.983	0.154
0.46	39.1	396.1	0.0987	0.970	1.470	0.1512	1.528	0.993	0.1458	6.3	398.7	0.984	0.150

COMPUTATION SHEET STEADY STATE FLOW COEFFICIENTS

Figure 8 Cylinder Liner

Position	ΔP_o	P_1	$\Delta P_o/P_1$	Y	$\sqrt{P_1/T_1 \Delta P_o}$	$\dot{M}$	$R_d x10^{-5}$	K/K_m	$\dot{M}_{cor}$	ΔP_i	P_2	P_2/P_a	ϕ
0	44.9	401	0.1118	0.966	1.588	0.1625	1.64	0.993	0.1611	1.2	403.8	0.995	0.085
0.20	44.8	401	0.1116	0.966	1.586	0.1625	1.64	0.993	0.1611	1.1	403.9	0.995	0.085
0.30	44.5	400.8	0.1100	0.967	1.582	0.1624	1.64	0.993	0.1610	1.4	403.6	0.995	0.085
0.40	43.7	400.1	0.1092	0.967	1.560	0.160	1.618	0.993	0.1588	2.2	402.8	0.992	0.105
0.50	42.0	398.7	0.1051	0.968	1.530	0.157	1.585	0.993	0.1558	3.7	401.3	0.990	0.126
0.60	38.5	395.5	0.0975	0.970	1.460	0.1502	1.518	0.993	0.1492	7.0	398.0	0.981	0.162
0.65	34.6	392.0	0.0883	0.973	1.378	0.141	1.425	0.994	0.1402	10.8	394.2	0.974	0.190
0.70	26.6	385.2	0.0691	0.979	1.20	0.1247	1.260	0.994	0.1238	18.0	387.0	0.955	0.258
0.75	16.1	376.5	0.0428	0.987	0.922	0.0965	0.974	0.995	0.0962	27.7	375.3	0.925	0.315
0.80	5.6	368.1	0.0152	0.995	0.536	0.0565	0.571	0.999	0.0564	36.4	368.6	0.910	0.348
0.90	1.2	365.1	0.0028	1.0	0.247	0.0254	0.256	1.0	0.0255	39.9	365.1	0.900	0.356

SUMMARY SHEET - FLOW COEFFICIENTS

	Series 71		Series 71T		Figure 8 liner		
Lift	CA	CA/A_P	CA	CA/A_P	Position	CA	CA/A_P
0	0		0		0	3.24	0.2290
0.05	0.315	0.0223	0.564	0.0399	0.20	3.24	0.2290
0.10	0.609	0.0431	1.03	0.0728	0.30	3.23	0.2281
0.15	0.922	0.0651	1.368	0.0966	0.40	2.58	0.1825
0.20	1.13	0.0799	1.70	0.1201	0.50	2.11	0.1490
0.25	1.31	0.0925	1.814	0.1281	0.60	1.576	0.1114
0.30	1.475	0.1041	2.03	0.1435	0.65	1.262	0.0893
0.35	1.526	0.1078	2.14	0.1512	0.70	0.821	0.0580
0.40	1.570	0.1110	2.26	0.1598	0.75	0.521	0.0368
0.45	1.612	0.1140	2.27	0.1603	0.80	0.277	0.0196
0.46	1.661	0.1175			0.90	0.122	0.0086

OPERATIONAL DATA SHEET

NOZZLE : 0.05

Run	T_j	P_{oil}	P_1	P_i	$\triangle P$	T_1	P_E	T_E	P_T	Roto	B.L.	T	P_{atm}
51	180	47	31.7	30.1	23	78	4.2	508	0.15	12.45	15.7	5.55	30.09
53	180	47	30.1	28.65	23	80	4.05	450	0.15	11.2	12.3	5.25	30.09
55	180	47	28.4	26.9	23	80	3.7	390	0.15	10.3	8.7	4.80	30.09
57	180	47	27.7	26.0	23	81	3.4	342	0.15	9.3	5.9	4.50	30.09
59	180	47	26.1	24.5	23	81	3.1	290	0.15	7.9	1.4	4.10	30.09
61	180	47	26.1	24.9	18	82	3.4	545	0.15	12.2	14.9	4.57	30.09
63	180	47	24.6	23.4	18	82	3.1	490	0.15	11.05	11.7	4.25	30.09
65	180	47	23.65	22.3	18	82	2.9	428	0.15	10.15	8.7	4.00	30.09
67	180	47	22.8	21.6	18	82	2.7	378	0.15	9.1	5.85	3.72	30.09
69	180	47	21.3	20.1	18	82	2.45	300	0.15	7.45	1.35	3.37	30.09
71	180	47	20.58	19.7	13	83	2.6	650	0.15	12.0	14.45	3.70	29.96
73	180	47	19.4	18.5	13	83	2.40	572	0.15	10.95	11.6	3.40	29.96
75	180	47	18.7	17.8	13	83	2.25	502	0.15	10.1	9.1	3.20	29.96
77	180	47	18.0	17.1	13	83	2.1	442	0.15	9.15	6.02	3.07	29.96
79	180	47	17.0	16.05	13	83	2.0	357	0.15	7.8	2.12	3.00	29.96
81	180	47	14.7	14.2	8	83	1.95	785	0.15	12.1	13.52	2.72	29.96
83	180	47	14.0	13.5	8	83	2.0	692	0.15	11.1	11.65	2.50	29.96
85	180	47	14.35	13.75	8	82	1.85	612	0.15	10.1	9.1	2.32	29.96
87	180	47	12.8	12.2	8	81	1.7	530	0.15	9.05	6.2	2.10	29.96
89	180	47	11.65	11.1	8	81	1.55	435	0.15	7.8	2.9	1.90	29.96

COMPUTATION SHEET

NOZZLE : 0.05

Run	P'_w	P/P'_w	Y	$\dot{M}_c$ factor	$\dot{M}_{chart}$	$\dot{M}_a$	P_{Ea}	ρ_s	R_s	η_s	Γ	$\dot{M}_f$	F
51	839	0.0274	0.992	1.427	0.1128	0.1596	34.29	0.0846	2.17	0.920	0.424	0.00265	0.0392
53	819	0.0282	0.992	1.420	0.1128	0.1589	34.14	0.0839	2.18	0.920	0.422	0.00220	0.0328
55	795	0.0290	0.991	1.396	0.1128	0.1560	33.79	0.0830	2.16	0.920	0.426	0.00192	0.0289
57	785	0.0293	0.991	1.382	0.1128	0.1548	33.49	0.0822	2.16	0.920	0.426	0.00162	0.0246
59	764	0.0302	0.991	1.369	0.1128	0.1530	33.19	0.0814	2.16	0.920	0.426	0.00122	0.0187
61	764	0.0236	0.993	1.370	0.0998	0.1359	33.49	0.0819	1.93	0.913	0.473	0.00255	0.0397
63	744	0.0242	0.993	1.350	0.0998	0.1339	33.19	0.0811	1.90	0.910	0.480	0.00215	0.0335
65	726	0.0248	0.993	1.350	0.0998	0.1339	32.99	0.0806	1.91	0.911	0.477	0.00187	0.0293
67	719	0.0250	0.992	1.328	0.0998	0.1315	32.79	0.0802	1.89	0.909	0.481	0.00155	0.0239
69	697	0.0258	0.991	1.310	0.0998	0.1298	32.54	0.0795	1.875	0.908	0.484	0.00110	0.0175
71	701	0.01854	0.995	1.293	0.0848	0.1091	32.56	0.0795	1.58	0.866	0.548	0.00247	0.0413
73	698	0.01864	0.994	1.291	0.0848	0.1090	32.36	0.0791	1.59	0.8675	0.546	0.00212	0.0356
75	676	0.0192	0.994	1.282	0.0848	0.1082	32.21	0.0787	1.58	0.866	0.548	0.00185	0.0312
77	652	0.0199	0.994	1.272	0.0848	0.1073	32.06	0.0782	1.58	0.866	0.548	0.00157	0.0267
79	638	0.0204	0.994	1.248	0.0848	0.1052	31.96	0.0780	1.55	0.860	0.555	0.00120	0.0205
81	608	0.01318	0.996	1.218	0.0665	0.0806	31.91	0.0780	1.19	0.7675	0.645	0.00252	0.0485
83	598	0.01338	0.996	1.208	0.0665	0.0800	31.96	0.0780	1.18	0.764	0.647	0.00217	0.0419
85	603	0.01329	0.996	1.210	0.0665	0.0803	31.81	0.0779	1.11	0.740	0.666	0.00185	0.0344
87	581	0.01376	0.996	1.191	0.0665	0.0790	31.66	0.0776	1.17	0.761	0.651	0.00155	0.0301
89	566	0.01414	0.996	1.179	0.0665	0.0782	31.51	0.0773	1.14	0.751	0.659	0.00120	0.0234

COMPUTATION SHEET

NOZZLE : 0.05

Run	B.L.	$BMEP_M$	IMEP	$FMEP_M$	$FMEP_c$	$BMEP_c$
51	15.7	88.3	286	197.7	65.9	220.1
53	12.3	69.1	265.5	196.4	65.5	200.0
55	8.7	48.8	229.5	180.7	60.2	169.3
57	5.9	33.2	218.5	185.3	61.8	156.7
59	1.4	7.87	175.5	167.6	59.2	116.3
61	14.9	83.8	268	184.2	61.4	206.6
63	11.7	65.8	240	174.2	58.1	181.9
65	8.7	48.8	218.5	169.7	56.6	161.9
67	5.85	32.9	197	164.1	54.7	142.3
69	1.35	7.59	148	140.4	46.8	101.2
71	14.45	81.2	258	176.8	58.9	199.1
73	11.6	65.2	227	161.8	53.9	173.1
75	9.1	51.1	217.5	166.4	55.5	162.0
77	6.02	33.8	187.5	153.7	51.2	136.3
79	2.12	11.9	157.5	145.6	38.5	119.0
81	13.52	76.1	243	166.9	56.0	187.0
83	11.65	65.5	222	156.5	52.2	169.8
85	9.1	51.1	205	153.9	51.3	153.7
87	6.2	34.8	179	144.2	38.1	140.9
89	2.9	16.3	158.5	142.2	37.4	121.1

OPERATIONAL DATA SHEET

NOZZLE : 0.025

Run	T_j	P_{oil}	P'	P_i	ΔP	T'	P_E	T_E	P_T	Roto	B.L.	T	P_{atm}
3	180	46	23.6	23	10.4	71	5.1	640	0.2	11.7	9.7	3.35	29.21
5	175	47	23.8	23	12.4	71	4.6	468	0.2	10.0	5.7	3.35	29.21
7	175	47	23.9	23	13.6	71	4.9	390	0.2	9.25	3.4	3.40	29.21
9	170	47	23.95	23	14.8	71	5.1	325	0.2	8.2	0.75	3.37	29.21
11	170	47	18.45	18	6.8	71	3.15	735	0.2	11.45	9.1	2.45	29.21
13	175	47	18.55	18	7.9	72	3.8	560	0.2	10.0	5.9	2.5	29.21
15	175	47	18.55	18	8.75	72	3.8	475	0.2	9.1	4.15	2.52	29.21
17	175	47	18.65	18	9.85	72	4.0	390	0.2	8.15	1.95	2.55	29.21
19	180	47	13.25	13	3.2	71	2.9	825	0.2	11.5	7.50	1.65	29.21
21	180	47	13.25	13	4.0	71	3.5	700	0.2	10.1	6.15	1.70	29.21
23	180	47	13.3	13	4.85	71	3.1	555	0.2	9.1	3.95	1.70	29.21
25	180	47	13.4	13	5.6	70	3.25	438	0.2	8.0	1.85	1.72	29.21
27	180	47	10.15	10	2.3	70	2.7	800	0.2	11.1	5.25	1.25	29.21
29	180	47	10.15	10	2.5	70	2.7	765	0.2	10.3	5.05	1.25	29.21
31	180	47	10.15	10	3.0	70	2.85	624	0.2	9.1	3.50	1.25	29.21
33	175	47	10.25	10	3.7	70	2.85	480	0.2	7.9	1.2	1.25	29.21

COMPUTATION SHEET

NOZZLE : 0.025

Run	P_{iw}	P/P_{iw}	Y	$\dot{M}_c$ Factor	$\dot{M}_{chart}$	$\dot{M}_a$	P_{Ea}	ρ_s	R_s	η_s	Γ	$\dot{M}_f$	F
3	718	0.0145	0.9958	1.340	0.0758	0.1014	34.31	0.0855	1.365	0.818	0.599	0.0024	0.0395
5	721	0.0172	0.9949	1.341	0.0828	0.1106	33.81	0.0856	1.485	0.847	0.571	0.0019	0.0301
7	723	0.01884	0.9944	1.342	0.0867	0.1158	34.11	0.0858	1.551	0.860	0.554	0.00165	0.0257
9	723	0.0204	0.994	1.342	0.0908	0.1210	34.31	0.0859	1.62	0.876	0.541	0.00132	0.0202
11	649	0.01048	0.9969	1.270	0.0612	0.0774	32.36	0.0806	1.105	0.741	0.670	0.00232	0.0448
13	650	0.01214	0.9953	1.270	0.0660	0.0835	33.01	0.0823	1.167	0.760	0.652	0.00185	0.0340
15	650	0.01345	0.996	1.270	0.0695	0.0880	33.01	0.0823	1.229	0.780	0.635	0.00158	0.0291
17	650	0.01515	0.9955	1.275	0.0738	0.0934	33.21	0.0828	1.297	0.800	0.617	0.00130	0.0226
19	576	0.00555	0.9983	1.201	0.0422	0.0506	32.11	0.0802	0.725	0.593	0.818	0.00232	0.0560
21	576	0.00698	0.998	1.201	0.0472	0.0566	32.71	0.0817	0.795	0.622	0.783	0.00189	0.0426
23	579	0.00839	0.997	1.202	0.0578	0.0621	32.31	0.0807	0.885	0.657	0.743	0.0016	0.0347
25	580	0.00965	0.997	1.202	0.0557	0.0668	32.46	0.0813	0.945	0.680	0.720	0.0013	0.0270
27	535	0.00431	0.999	1.155	0.0360	0.0415	31.91	0.0799	0.597	0.533	0.892	0.0022	0.0595
29	535	0.00467	0.999	1.155	0.0373	0.0430	31.91	0.0799	0.619	0.543	0.878	0.00193	0.0512
31	535	0.00561	0.998	1.155	0.0410	0.0473	32.06	0.0802	0.678	0.571	0.844	0.00158	0.0396
33	536	0.0069	0.998	1.158	0.0453	0.0524	32.06	0.0802	0.749	0.602	0.804	0.00128	0.0304

COMPUTATION SHEET

NOZZLE : 0.025

Run	B.L.	$BMEP_M$	IMEP	$FMEP_M$	$FMEP_c$	$BMEP_c$
3	9.7	54.5	227	172.5	57.5	169.5
5	5.7	32.0	192	160.0	53.3	138.7
7	3.4	19.1	196	176.9	59.0	137.0
9	0.75	4.22	161	156.8	52.3	108.7
11	9.1	51.1	221	169.9	56.6	164.4
13	5.9	33.2	190	156.8	52.3	137.7
15	4.15	23.3	181.5	158.2	52.7	128.8
17	1.95	10.95	143	132.0	41.3	101.7
19	7.5	42.2	187.5	145.3	48.4	139.1
21	6.15	34.5	184	149.5	39.8	144.2
23	3.95	22.0	152.5	130.5	43.5	109.0
25	1.85	10.4	143	132.6	43.2	99.8
27	5.25	29.5	168	138.5	46.2	121.8
29	5.05	28.4	160	131.6	43.9	116.1
31	3.5	19.65	148	128.4	42.8	105.2
33	1.2	6.75	122.5	115.75	38.6	83.9

DATA SHEET

COMPARISON OF EFFECTIVE EXHAUST-GAS VELOCITY

NOZZLE : 0.20 $A_n = 2.83 \text{ in}^2$

Run*	P_t	$\dot{M}_T$	T	u	T_E	a_E	u/a_E	$\frac{P_t A_n g_o}{\dot{M}_T a_E}$
10	29.75	0.1326	3.03	736	960	1519	0.484	6.59
9	29.60	0.0899	1.79	642	991	1542	0.416	9.54
14	29.70	0.1077	2.75	823	1204	1700	0.484	7.26
13	29.75	0.1310	3.43	844	1075	1606	0.525	6.34
15	29.60	0.0906	2.57	911	1335	1790	0.509	8.18
3	29.75	0.1326	2.71	661	832	1415	0.467	7.09
6	29.65	0.1067	2.11	638	940	1501	0.425	8.30
11	29.65	0.1086	2.53	751	1058	1592	0.471	7.67
12	29.60	0.0916	2.07	727	1142	1658	0.438	8.95
			NOZZLE : 0.10		$A_n = 1.415 \text{ in}^2$			
66	30.30	0.1329	4.07	985	1122	1641	0.600	3.10
76	30.10	0.0894	2.64	959	1341	1799	0.534	4.34
123	30.40	0.1100	3.07	900	1057	1593	0.565	3.95
64	30.25	0.1303	3.36	829	864	1440	0.576	3.61
65	30.30	0.1342	3.71	890	992	1544	0.576	3.27
70	30.15	0.1102	2.89	844	1058	1593	0.530	3.84
71	30.15	0.1098	3.29	964	1213	1714	0.563	3.54
74	30.05	0.0861	1.96	755	982	1538	0.491	4.99
125	30.50	0.1328	4.14	1000	1101	1629	0.614	3.11

*Run numbers refer to Ref.(2), from which operational data were taken.

DATA SHEET

COMPARISON OF EFFECTIVE EXHAUST-GAS VELOCITY

NOZZLE : 0.05 $A_n = 0.707$ in^2

Run	P_t	M_T	T	u	T_E	a_E	u/a_E	$\frac{P_t A_n g_o}{M_T a_E}$
51	30.29	0.1623	5.55	1037	968	1521	0.680	1.37
53	30.29	0.1611	5.25	1017	910	1478	0.689	1.42
55	30.29	0.1579	4.80	980	850	1428	0.682	1.50
57	30.29	0.1564	4.50	926	802	1390	0.666	1.56
59	30.29	0.1542	4.10	855	750	1342	0.636	1.63
61	30.29	0.1385	4.57	1062	1005	1553	0.684	1.57
63	30.29	0.1361	4.25	1012	950	1511	0.665	1.64
65	30.29	0.1357	4.00	951	888	1460	0.651	1.72
67	30.29	0.1331	3.72	898	838	1418	0.634	1.80
69	30.29	0.1309	3.37	831	760	1351	0.615	1.92
71	30.16	0.1116	3.70	1088	1110	1631	0.665	1.86
73	30.16	0.1111	3.40	985	1032	1535	0.642	1.98
75	30.16	0.1101	3.20	936	962	1518	0.616	2.02
77	30.16	0.1089	3.07	909	902	1472	0.616	2.11
79	30.16	0.1064	3.00	909	817	1401	0.647	2.26
81	30.16	0.0831	2.72	1052	1245	1703	0.607	2.38
83	30.16	0.0822	2.50	978	1152	1663	0.588	2.48
85	30.16	0.0822	2.32	911	1072	1608	0.567	2.57
87	30.16	0.0806	2.10	838	990	1542	0.543	2.71
89	30.16	0.0794	1.90	771	895	1469	0.526	2.93

DATA SHEET

COMPARISON OF EFFECTIVE EXHAUST-GAS VELOCITY

NOZZLE : 0.025 $A_n = 0.3535$ in^2

Run	P_t	M_T	T	u	T_E	a_E	u/a_E	$\frac{P_t A_n g_o}{M_T a_E}$
3	29.41	0.1038	3.35	1040	1100	1629	0.640	0.964
5	29.41	0.1125	3.35	958	928	1493	0.641	0.964
7	29.41	0.1175	3.40	933	850	1430	0.652	0.964
9	29.41	0.1223	3.37	888	785	1374	0.646	0.964
11	29.41	0.0797	2.45	990	1195	1692	0.584	1.24
13	29.41	0.0854	2.50	944	1020	1568	0.602	1.20
15	29.41	0.0896	2.52	905	935	1499	0.604	1.24
17	29.41	0.0947	2.53	860	850	1430	0.601	1.21
19	29.41	0.0529	1.65	1005	1285	1760	0.572	1.76
21	29.41	0.0585	1.70	935	1160	1670	0.560	1.68
23	29.41	0.637	1.70	859	1015	1562	0.549	1.58
25	29.41	0.0681	1.72	814	898	1468	0.554	1.64
27	29.41	0.0437	1.25	921	1260	1740	0.529	2.18
29	29.41	0.0449	1.25	898	1225	1716	0.523	2.14
31	29.41	0.0489	1.25	825	1084	1616	0.511	2.08
33	29.41	0.0537	1.25	750	940	1504	0.499	2.04

DATA SHEET

THRUST AND IMEP RELATION

NOZZLE : 0.05

Run	T_E	a_E	M_T	IMEP	T	$\frac{T\ g_o}{M_T a_E}$	W
51	968	1521	0.1623	286	5.55	0.680	526
53	910	1478	0.1611	265.5	5.25	0.689	506
55	850	1428	0.1579	229.5	4.80	0.682	464
57	802	1390	0.1564	218.5	4.50	0.666	458
59	750	1342	0.1542	175.5	4.10	0.636	384
61	1005	1553	0.1385	268	4.57	0.684	566
63	950	1511	0.1361	240	4.25	0.665	531
65	888	1460	0.1357	218.5	4.00	0.651	502
67	838	1418	0.1331	197	3.72	0.634	475
69	760	1351	0.1309	148	3.37	0.615	381
71	1110	1631	0.1116	258	3.70	0.665	645
73	1032	1535	0.1111	227	3.40	0.642	606
75	962	1518	0.1101	217.5	3.20	0.616	592
77	902	1472	0.1089	187.5	3.07	0.616	531
79	817	1401	0.1064	157.5	3.00	0.647	480
81	1245	1730	0.0831	243	2.72	0.607	768
83	1152	1663	0.0822	222	2.50	0.588	739
85	1072	1608	0.0822	205	2.32	0.567	705
87	990	1542	0.0806	179	2.10	0.543	652
89	895	1469	0.0794	158.5	1.90	0.526	620

$$W = \frac{IMEP \times A_p \times g_o}{M_T \times a_E}$$

DATA SHEET

THRUST AND IMEP RELATION

NOZZLE : 0.025

Run	T_E	a_E	M_T	IMEP	T	$\frac{T\ g_o}{M_T a_E}$	W
3	1100	1629	0.1038	227	3.35	0.640	611
5	928	1493	0.1125	192	3.35	0.641	520
7	850	1430	0.1175	196	3.40	0.652	532
9	785	1374	0.1223	161	3.37	0.646	435
11	1195	1692	0.0797	221	2.45	0.584	745
13	1020	1568	0.0854	190	2.50	0.602	645
15	935	1499	0.0896	181.5	2.52	0.604	615
17	850	1430	0.0947	143	2.53	0.601	480
19	1285	1760	0.0529	187.5	1.65	0.572	915
21	1160	1670	0.0585	184	1.70	0.560	856
23	1015	1562	0.0637	152.5	1.70	0.549	696
25	898	1468	0.0681	143	1.72	0.554	650
27	1260	1740	0.0437	168	1.25	0.529	1008
29	1225	1716	0.0449	160	1.25	0.523	1008
31	1084	1616	0.0489	148	1.25	0.511	851
33	940	1504	0.0537	122.5	1.25	0.499	689

COMPUTATION SHEET
MEP RELATIONS
NOZZLE : 0.05

Run	F	$F' = \Gamma F$	$1 + F'$	u^2	$\frac{tmep}{imep}$	imep	tmep	$\frac{imep + tmep}{imep}$	R_s	P_e/P_i	W
51	0.0392	0.0166	1.017	1.038×10^6	0.112	286	32.0	1.111	2.17	0.504	526
53	0.0328	0.0138	1.014	1.014x	0.131	265.5	34.8	1.142	2.18	0.516	506
55	0.0289	0.0123	1.012	0.958	0.141	229.5	32.4	1.140	2.16	0.532	464
57	0.0246	0.0105	1.011	0.853	0.145	218.5	31.7	1.093	2.16	0.540	458
59	0.0187	0.00795	1.008	0.730	0.163	179.5	29.2	1.164	2.16	0.554	384
61	0.0397	0.0188	1.019	1.06	0.101	268	27.0	1.10	1.93	0.551	566
63	0.0335	0.0161	1.016	1.01	0.112	240	26.9	1.112	1.90	0.562	531
65	0.0293	0.0140	1.014	0.921	0.118	218	25.7	1.116	1.91	0.579	502
67	0.0239	0.0115	1.012	0.812	0.126	197	24.8	1.126	1.89	0.586	475
69	0.0175	0.0085	1.009	0.688	0.145	148	21.4	1.142	1.875	0.604	381
71	0.0413	0.0226	1.023	1.09	0.0870	258	22.4	1.089	1.58	0.609	645
73	0.0356	0.0194	1.019	0.968	0.0885	227	20.1	1.089	1.59	0.624	606
75	0.0312	0.0171	1.017	0.872	0.0913	217.5	19.8	1.090	1.58	0.634	592
77	0.0267	0.0146	1.015	0.821	0.1009	187.5	18.8	1.111	1.58	0.643	531
79	0.0205	0.0114	1.011	0.821	0.130	157.5	20.5	1.129	1.55	0.658	480
81	0.0485	0.0311	1.031	1.051	0.0616	243	15.0	1.061	1.19	0.686	768
83	0.0419	0.0271	1.027	0.938	0.0625	222	13.9	1.061	1.18	0.697	739
85	0.0344	0.0229	1.023	0.829	0.0648	205	13.3	1.064	1.11	0.693	705
87	0.0301	0.0196	1.020	0.700	0.0640	179	11.5	1.063	1.17	0.718	652
89	0.0234	0.0154	1.015	0.591	0.0686	158.5	10.9	1.067	1.14	0.739	620

COMPUTATION SHEET
MEP RELATIONS
NOZZLE : 0.025

Run	F	$F' = \Gamma F$	$1 + F'$	u^2	$\frac{tmep}{imep}$	imep	tmep	$\frac{imep + tmep}{imep}$	R_s	P_e/P_i	W
3	0.0395	0.0236	1.0236	1.036×10^6	0.079	227.0	17.9	1.078	1.365	0.564	611
5	0.0301	0.0172	1.0172	0.908	0.094	192.0	17.9	1.092	1.485	0.564	520
7	0.0257	0.0142	1.0142	0.860	0.108	196.0	21.2	1.109	1.551	0.564	532
9	0.0202	0.0109	1.0109	0.790	0.129	161.0	20.8	1.128	1.62	0.564	435
11	0.0448	0.0301	1.0301	0.968	0.0584	221.0	12.9	1.058	1.105	0.623	745
13	0.0340	0.0222	1.0222	0.880	0.0715	190	13.6	1.071	1.167	0.623	645
15	0.0291	0.0185	1.0185	0.810	0.0785	181.5	14.2	1.078	1.229	0.623	615
17	0.0226	0.0139	1.0139	0.731	0.0705	143.0	10.1	1.07	1.297	0.623	480
19	0.0560	0.0458	1.0458	1.002	0.0403	187.5	7.58	1.042	0.725	0.696	915
21	0.0426	0.0334	1.0334	0.870	0.0474	184.0	8.71	1.045	0.795	0.696	856
23	0.0347	0.0258	1.0258	0.731	0.0512	152.5	7.80	1.051	0.885	0.696	696
25	0.0270	0.0194	1.0194	0.660	0.0609	143.0	8.70	1.06	0.945	0.696	650
27	0.0595	0.0531	1.0531	0.848	0.0296	168.0	4.95	1.028	0.597	0.750	1008
29	0.0512	0.0450	1.0450	0.812	0.0332	160.0	5.32	1.034	0.619	0.750	1008
31	0.0396	0.0334	1.0334	0.679	0.0370	148.0	5.48	1.038	0.678	0.750	851
33	0.0304	0.0244	1.0244	0.560	0.0414	122.5	5.06	1.04	0.749	0.750	689

DATA SHEET
THRUST AND BRAKE POWER RELATION
NOZZLE 0.05

Run	T_1	a	a^2	M_c	$BMEP_c$	BHP	$\frac{P_{go}}{Ma^2}$	T	$\frac{T_{go}}{Ma}$	R_s	F/A
51	538	1134	1.285×10^6	0.1596	220.1	47.1	4.10	5.55	0.988	2.17	0.0392
53	540	1139	1.295×10^6	0.1589	200.	42.7	3.70	5.25	0.934	2.18	.0328
55	540	1139	1.295×10^6	.1560	169.3	36.1	3.19	4.80	0.870	2.16	.0289
57	541	1140	1.30×10^6	.1548	156.7	33.4	2.96	4.50	0.821	2.16	.0246
59	541	1140	1.30×10^6	.1530	116.3	24.8	2.22	4.10	0.757	2.16	.0187
61	542	1141	1.31×10^6	.1359	206.6	44.1	4.42	4.57	0.949	1.93	.0397
63	542	1141	1.31×10^6	.1339	181.9	38.8	3.94	4.25	0.895	1.90	.0335
65	542	1141	1.31×10^6	.1339	161.9	34.5	3.51	4.00	0.843	1.91	.0293
67	542	1141	1.31×10^6	.1315	142.3	30.4	3.15	3.72	0.799	1.89	.0239
69	542	1141	1.31×10^6	.1298	101.2	21.6	2.27	3.37	0.733	1.875	.0175
71	543	1142	1.31×10^6	.1091	199.1	42.5	5.30	3.70	0.955	1.580	.0413
73	543	1142	1.31×10^6	.1090	173.1	37.0	4.62	3.40	0.879	1.59	.0356
75	543	1142	1.31×10^6	.1082	162.0	34.6	4.35	3.20	0.833	1.58	.0312
77	543	1142	1.31×10^6	.1073	136.3	29.1	3.69	3.07	0.806	1.58	.0267
79	543	1142	1.31×10^6	.1052	119.0	25.4	3.29	3.00	0.803	1.55	.0205
81	543	1142	1.31×10^6	.0806	186.0	39.7	6.71	2.72	0.951	1.19	.0485
83	543	1142	1.31×10^6	.0800	169.8	36.2	6.16	2.50	0.881	1.18	.0419
85	542	1141	1.31×10^6	.0803	153.7	32.8	5.56	2.32	0.816	1.11	.0344
87	541	1140	1.30×10^6	.0790	140.9	30.5	5.29	2.10	0.752	1.17	.0301
89	541	1140	1.30×10^6	.0782	121.1	25.8	4.53	1.90	0.687	1.14	.0234

DATA SHEET
THRUST AND BRAKE POWER RELATION
NOZZLE 0.025

Run	T_1	a	a^2	M_c	$BMEP_c$	BHP	$\frac{Pg_o}{Ma^2}$	T	$\frac{Tg_o}{Ma}$	R_s	F/A
3	531	1131	1.28×10^6	.1014	169.5	36.2	4.97	3.35	0.939	1.365	.0395
5	531	1131	1.28×10^6	.1106	138.7	29.6	3.73	3.35	0.863	1.485	.0301
7	531	1131	1.28×10^6	.1158	137.0	29.2	3.52	3.4	0.836	1.551	.0257
9	531	1131	1.28×10^6	.1210	108.7	23.2	2.67	3.37	0.793	1.62	.0202
11	531	1131	1.28×10^6	.0774	164.4	35.1	6.33	2.45	0.901	1.105	.0448
13	532	1132	1.28×10^6	.0835	137.7	29.4	4.90	2.5	0.853	1.167	.0340
15	532	1132	1.28×10^6	.0880	128.8	27.4	4.34	2.52	0.812	1.229	.0291
17	532	1132	1.28×10^6	.0934	101.7	21.7	3.24	2.55	0.770	1.297	.0226
19	531	1131	1.28×10^6	.0506	139.1	29.7	8.17	1.65	0.928	0.725	.0560
21	531	1131	1.28×10^6	.0566	144.2	30.8	7.58	1.70	0.855	0.795	.0426
23	530	1129	1.28×10^6	.0621	109.0	23.3	5.24	1.70	0.780	0.885	.0347
25	530	1129	1.28×10^6	.0668	99.8	21.6	4.51	1.72	0.735	0.945	.0270
27	530	1129	1.28×10^6	.0415	121.8	26.0	8.75	1.25	0.858	0.597	.0595
29	530	1129	1.28×10^6	.0430	116.1	24.8	8.04	1.25	0.829	0.619	.0512
31	530	1129	1.28×10^6	.0473	105.2	22.5	6.62	1.25	0.754	0.678	.0396
33	530	1129	1.28×10^6	.0524	83.9	18.2	4.84	1.25	0.682	0.749	.0304
22	531	1131	1.28×10^6	.0550	122.4	26.1	6.62	1.67	0.864	0.777	.0426

APPENDIX D

SAMPLE CALCULATION

Run #51

Nozzle 0.05

P_a 30.09 "Hg

1. Calculation of Scavenging ratic (R_s)

a. Using the Leary and Tsai orifice analysis

$$\dot{M}_a = (\dot{M}_{chart}) \sqrt{\frac{P_1 \; P_a}{30.00} \times \frac{540}{T_1}} \qquad (Y)$$

for $\dot{M}_{chart}$ see figure VIII

for Y see figure IX

$$\dot{M}_a = (0.1128) \sqrt{\frac{30.1 + 30.09}{30.00} \times \frac{540}{538}} \times 0.992 = 0.1596$$

$$\dot{M}_a = 0.1596 \quad \#/sec$$

b. $$R_s = \frac{60\, \dot{M}_a}{\rho_s N V_c}$$

$N = 1200$ rpm

$V_c = 0.0435\ ft^3$

$$\rho_s \quad \frac{P_E}{RT_1}$$

$P_E = 34.29$ "H_g

$T_1 = 538$ R

$$R_s = \frac{60\, \dot{M}_a}{1200 \times 0.0435} = 1.15 \frac{\dot{M}_a}{\rho_s}$$

$$\rho_s = \frac{0.491 \times P_E \times 144}{53.3\ T_1} = 1.328 \frac{P_E}{T_1}$$

$$\rho_s = \frac{1.328 \times 34.29}{538} = 0.0846 \quad lbs/ft^3$$

$$R_s = \frac{1.15 \times 0.1596}{0.0846} = 2.17$$

Figure VIII

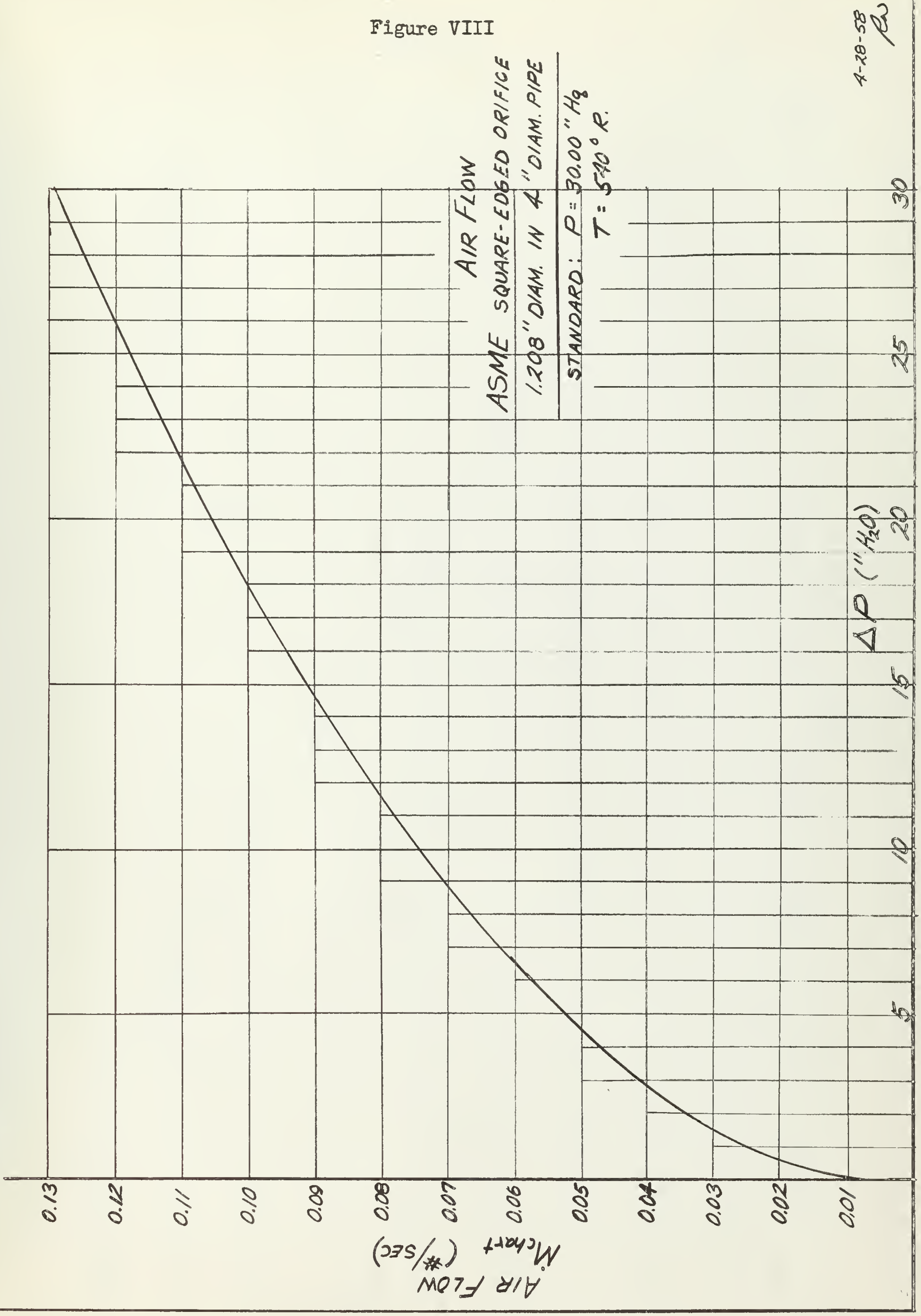
A-28-58
AIR FLOW
ASME SQUARE-EDGED ORIFICE
1.208" DIAM. IN 4" DIAM. PIPE
STANDARD: P = 30.00" Hg
T = 540° R.
ΔP ("H2O)
5
10
15
20
25
30
0.13
0.12
0.11
0.10
0.09
0.08
0.07
0.06
0.05
0.04
0.03
0.02
0.01
AIR FLOW
Ṁchart
(#/SEC)

Figure IX

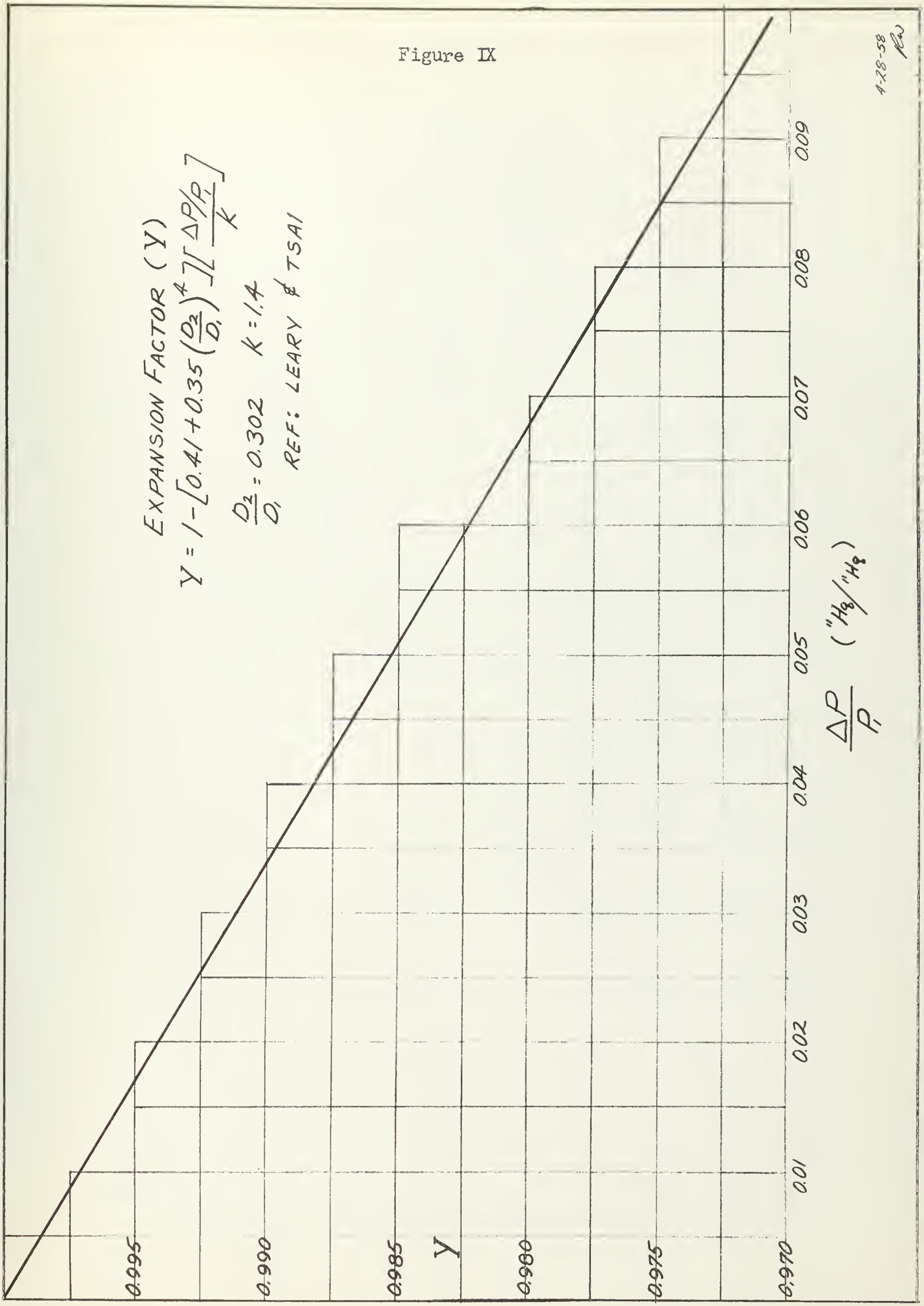
EXPANSION FACTOR (Y)
$Y = 1 - [0.41 + 0.35 (\frac{D_2}{D_1})^4][\frac{\Delta P/P_1}{k}]$
$\frac{D_2}{D_1} = 0.302$ $k = 1.4$
REF: LEARY & TSAI
4-28-58
Y
0.995
0.990
0.985
0.980
0.975
0.970
0.01
0.02
0.03
0.04
0.05
0.06
0.07
0.08
0.09
$\frac{\Delta P}{P_1}$ ("Hg/"Hg)

4-28-58 RW

Figure X

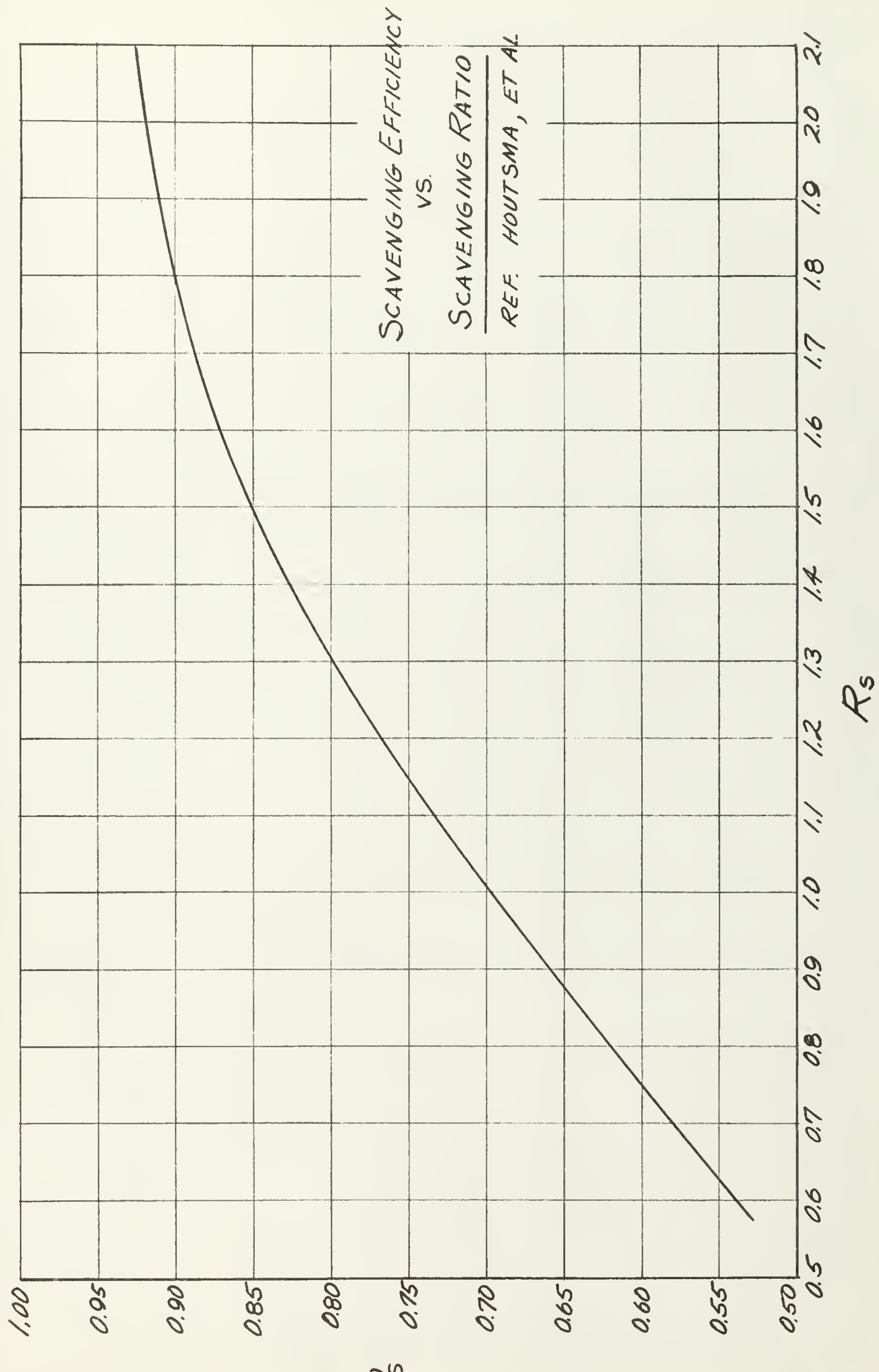

Figure XI

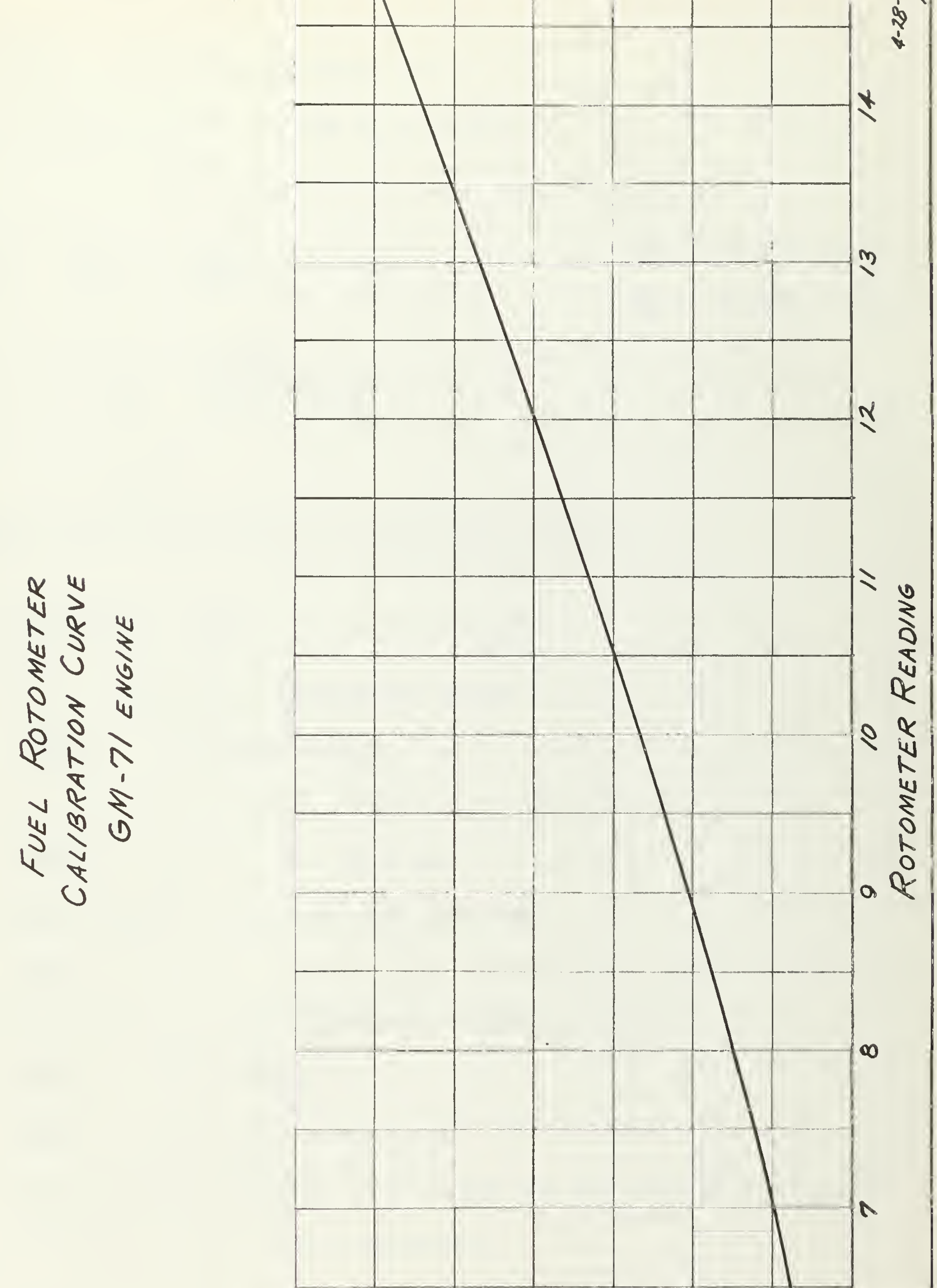

FUEL ROTOMETER
CALIBRATION CURVE
GM-71 ENGINE
ROTOMETER READING
6
7
8
9
10
11
12
13
14
FUEL FLOW, M_f (#/SEC)
0.001
0.002
0.003
0.004
0.005

2. Calculation of the fuel-air ratio (F)

a. Entering figure X with $R_s = 2.17$:

$$\eta_s = 0.92$$

b. $$\frac{\eta_s}{R_s} = \frac{0.92}{2.17} = 0.424$$

$\dot{M}_f = 0.00265$ lb/sec

$\dot{M}_a = 0.1596$ lb/sec

c. $$F = \frac{\dot{M}_f}{\dot{M}_a} = \frac{0.00265}{0.424 \times 0.1596}$$

$$F = 0.0392$$

3. Calculation of Brake mean effective pressure (BMEP)

a. Dynamometer $BMEP_M$

From evaluation of dynamometer system

$BMEP_M = 5.62$ (Brake load)

B.L. = 15.7 "Hg

$BMEP_M = 5.62 \times 15.7 = 88.3$ psi

b. IMEP was determined from indicator card

IMEP = 286 psi

c. Determination of friction mean effective pressure

$FMEP = IMEP - BMEP_M$

$FMEP = 286 - 88.3 = 197.7$ psi

However since the FMEP so determined was the total friction mean effective pressure for 3 cylinders

$FMEP_c = \frac{197.7}{3} = 65.9$ psi (for one cylinder)

d. Corrected value of BMEP

$BMEP_c = 286 - 65.9 = 220.1$ psi

4. Determination of the Pinkel factors for correlation of data with reference (5)

$$\dot{M}_T = \dot{M}_a + \dot{M}_f = 0.1596 + 0.00265 = 0.1623 \quad \text{lb/sec}$$

$$P_T = 14.88 \text{ psi}$$

$$A_N = 0.05 \, A_p$$

a. $u = \dfrac{T_{go}}{\dot{M}_T} = \dfrac{32.2 \times 5.55}{0.1623}$ $\qquad T = \dfrac{\text{Reading on manometer}}{2}$

$T = \dfrac{11.1}{2} = 5.55$

$$u = 1037.0 \text{ ft/sec}$$

$$T_E = 968^{o}R$$

$$a_E = 49 \sqrt{T_E} = 49 \sqrt{968} = 1521 \text{ ft/sec}$$

$$u/a_E = \frac{1037}{1521} = 0.680$$

b. $\dfrac{P_T A_N \, go}{M_T a_E} = \dfrac{14.88}{144} \times \dfrac{0.05 \times 14.15 \times 32.2}{0.1623 \times 1521}$

$$\frac{P_T A_N \, go}{M_T a_E} = 1.37$$

5. Determination of Thrust and IMEP relationships

It was attempted to correlate thrust as measured on the force plate to engine IMEP by the following dimensionless coefficients.

$$\frac{T_{go}}{M_T a_E} \quad \text{and} \quad \frac{\text{IMEP} \times A_p \times go}{M_T \times a_E}$$

$$T = 5.55 \text{ lbs}$$

$$\dot{M}_T = 0.1623 \text{ lb/sec}$$

$$a_E = 1521 \text{ ft/sec}$$

$$\text{IMEP} = 286 \text{ psi}$$

a. $\dfrac{T_{go}}{M_T a_E} = \dfrac{5.55 \times 32.2}{0.1623 \times 1521}$

$\dfrac{T_{go}}{M_T a_E} = 0.680$

b. $\dfrac{IMEP \times A_p \times g_o}{M_T \times a_E} = \dfrac{286 \times 14.15 \times 32.2}{0.1623 \times 1521} = 526$

6. Determination of TMEP and IMEP relationships

a. An analysis of the blowdown turbine process leads to the following expression

$$\frac{TMEP}{IMEP} = \frac{1 + F'}{Q_c F \eta'_i} \left\{ \frac{u^2 \eta_{kb}}{2 g_o J \Gamma} \right\}$$

b. F' (overall fuel-air ratio) $= \Gamma F$

$F' = 0.424 \times 0.0392 = 0.0166$

$Q_c = 18{,}500$ BTU/lb

$J = 778$ ft lb/BTU

$\eta_{kb} = 0.75$ (from NACA technical data)

$\eta'_i = 0.46$ reference (11)

$$\frac{\eta_{kb}}{Q_c \eta'_i 2 g_o J} = \frac{0.75}{0.46 \times 18{,}500 \times 2 \times 32.2 \times 778} = \frac{1}{568 \times 10^5}$$

It follows that

c. $\dfrac{TMEP}{IMEP} = \dfrac{1}{568 \times 10^5} \left\{ \dfrac{1+F'}{F'} \times u^2 \right\}$

$\dfrac{TMEP}{IMEP} = \dfrac{1}{568 \times 10^5} \left\{ \dfrac{1.0166}{.0166} \times 1521^2 \right\}$

$\dfrac{TMEP}{IMEP} = 0.112$

d. $\dfrac{TMEP + IMEP}{IMEP} = \dfrac{1 + 0.112}{1} = 1.112$

$TMEP = 0.112(286) = 32.0$ psi

7. Determination of thrust and brake horsepower relations

a. $BHP = \frac{1.2}{5.62} \; BMEP_c = 0.2135 \; BMEP_c$

$BMEP_c = 220.1$ psi

$BHP = 0.2135\,(220.1) = 47.1$ hp

b. Thrust and brake horsepower are correlated on the basis of the following dimensionless coefficients:

$$\frac{\mathbb{P}_{go}}{M_a^{\,2}} \; ; \qquad \frac{T_{go}}{M_a} \; , \qquad R_s \text{ and } F \, .$$

c. Calculation of $\frac{\mathbb{P}_{go}}{M_a^{\,2}}$ and $\frac{T_{go}}{M_a}$

$$T_1 = 538^{\circ}R$$

$$a = 49\sqrt{T_1} = 49\sqrt{538} = 1134 \text{ ft/sec}$$

$$a^2 = (1.134 \times 10^3)^2 = 1.285 \times 10^6 \text{ ft}^2/\text{sec}^2$$

$$\dot{M}_a = 0.1596 \text{ lb/sec}$$

$$\mathbb{P} = 47.1 \text{ hp}$$

$$\frac{\mathbb{P}_{go}}{M_a^{\,2}} = \frac{1.782 \quad BHP}{M \quad a^2} \times 10^4$$

$$= \frac{1.782 \times 471.1}{0.1596 \times 1.285} \times 10^{-2} = 4.10$$

$$\frac{\mathbb{P}_{go}}{M_a^{\,2}} = 4.10$$

$$\frac{T_{go}}{M_a} = \frac{5.55 \times 32.2}{0.1596 \times 1134} = 0.988$$

$$F = 0.0392$$

$$R_s = 2.17$$

APPENDIX E

ENGINE FRICTION

Measurements of dynamometer brake load were made while running the engine under the various load operating conditions. Also, for each test run at these conditions, a pressure-time indicator diagram was taken using the MIT high speed pressure indicator apparatus. This diagram was further translated into a p-v indicator card for the determination of indicated mean effective pressure (IMEP) of the single cylinder.

Using this IMEP and the overall brake MEP determined from the brake load measurement, a value of overall friction MEP was obtained from $IMEP - BMEP_M = FMEP$. This overall FMEP was then divided by three to obtain approximately the single cylinder FMEP. By plotting these values of FMEP versus IMEP, no definite conclusions could be established in regard to correlations of same nozzle area, constant scavenge ratio, or fuel-air ratio. A qualitative mean line was established for comparative purposes. See figure XII.

It follows that the single cylinder BMEP may be determined from $IMEP_c - FMEP_c = BMEP_c$.

Figure XII

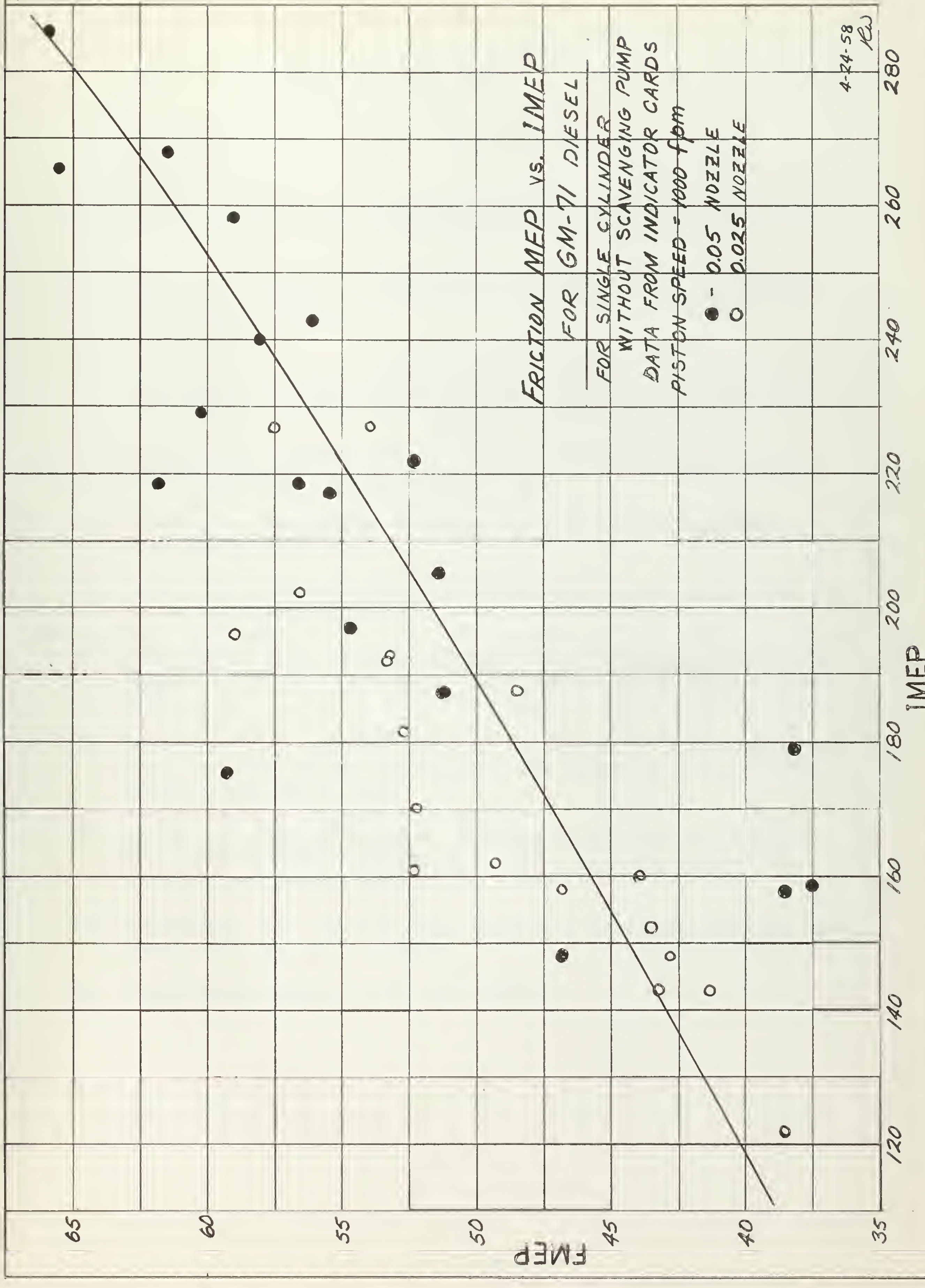
FRICTION MEP VS. IMEP
FOR GM-71 DIESEL
FOR SINGLE CYLINDER
WITHOUT SCAVENGING PUMP
DATA FROM INDICATOR CARDS
PISTON SPEED = 1000 fpm
● - 0.05 NOZZLE
○ 0.025 NOZZLE
4-24-58
IMEP
120
140
160
180
200
220
240
260
280
FMEP
65
60
55
50
45
40
35

APPENDIX F

BIBLIOGRAPHY

1. Parsons, T.M. and A. Zang, Measurement of the Available Energy in the Exhaust Gas of a Diesel Engine With Regard to Turbo-charging Application; BS Thesis, MIT Library, May 1952.

2. Crowley, J.D., A.W. Gottschalk, W.R. Nodell, The Utilization of Exhaust Gas Energy of a Two-stroke Diesel Engine; NavE Thesis, MIT Library, May 1957.

3. Taylor, C.F. et al, Loop Scavenging vs. Through Scavenging of the Two-cycle Engine; SAE Paper #247 presented at the SAE National Diesel Engine Meeting, Cleveland, Ohio, Nov. 5-6, 1957.

4. Leary, W.A. and D.H. Tsai, Metering of Gases by means of ASME Square Edge Orifice with Flange Taps.

5. Pinkel, B., Utilization of Exhaust Gas of Aircraft Engines; Tran SAE 54 (1946)714.

6. Smith, H.T., Turbocharging the Two-stroke Diesel Engine; SAE Journal 63 (June 1955)75.

7. Chamberlain, C.A. and G.H. Bollman, Turbocharging Two-stroke Gas Engines; ASME (OGP Division) Proceedings 26th Conference, June 1954.

8. Livengood, J.C. and J.D. Stanitz, The Effect of Inlet-valve Design, Size, and Lift on the Air Capacity and Output of a Four-stroke Engine; NACA TN915, 1943.

9. Turner, L.R. and R.N. Noyes, Performance of Composite Engine Consisting of Reciprocating Engine(SI), Blowdown Turbine and Steady-flow Turbine; NACA TN1447, 1947.

10. Schweitzer, P.H. and T.C. Tsu, Energy in the Engine Exhaust; ASME Trans, vol. 71, no. 6 (1949).

11. Class Notes, Course 2.797, MIT (1957).